

UNADJUSTED HAMILTONIAN MCMC WITH STRATIFIED MONTE CARLO TIME INTEGRATION

BY NAWAF BOU-RABEE^{1,a}, AND MILO MARSDEN^{2,b}

¹*Department of Mathematical Sciences
Rutgers University Camden
311 N 5th Street
Camden, NJ 08102 USA*, ^anawaf.bourabee@rutgers.edu

²*Department of Mathematics
Stanford University
450 Jane Stanford Way
Stanford, CA 94025 USA*, ^bmmarsden@stanford.edu

A randomized time integrator is suggested for unadjusted Hamiltonian Monte Carlo (uHMC) which involves a very minor modification to the usual Verlet time integrator, and hence, is easy to implement. For target distributions of the form $\mu(dx) \propto e^{-U(x)} dx$ where $U : \mathbb{R}^d \rightarrow \mathbb{R}_{\geq 0}$ is K -strongly convex but only L -gradient Lipschitz, and initial distributions ν with finite second moment, coupling proofs reveal that an ε -accurate approximation of the target distribution in L^2 -Wasserstein distance \mathcal{W}^2 can be achieved by the uHMC algorithm with randomized time integration using $O\left((d/K)^{1/3}(L/K)^{5/3}\varepsilon^{-2/3}\log(\mathcal{W}^2(\mu,\nu)/\varepsilon)^+\right)$ gradient evaluations; whereas for such rough target densities the corresponding complexity of the uHMC algorithm with Verlet time integration is in general $O\left((d/K)^{1/2}(L/K)^2\varepsilon^{-1}\log(\mathcal{W}^2(\mu,\nu)/\varepsilon)^+\right)$. Metropolis-adjustable randomized time integrators are also provided.

1. Introduction. Hamiltonian Monte Carlo (HMC) is a gradient-based MCMC method aimed at target probability distributions of the form $\mu(dx) \propto e^{-U(x)} dx$ where $U : \mathbb{R}^d \rightarrow \mathbb{R}_{\geq 0}$ is continuously differentiable. A defining characteristic of HMC is that it incorporates a measure-preserving Hamiltonian flow per transition step [18, 37]. This flow is typically approximated using a *deterministic* time integrator, and the discretization bias can either be borne (*unadjusted* HMC or *uHMC* for short) or eliminated by a Metropolis-Hastings filter (*adjusted* HMC).

In this work, *randomized* time integrators are developed for unadjusted HMC, which improve upon the current state of the art for *rough target densities* [42]. That is, we consider the case where U is assumed differentiable with L -Lipschitz gradient. But, crucially, we do not assume any regularity beyond this and in particular do not assume a Lipschitz Hessian.

Furthermore, we assume throughout this paper that U is K -strongly convex and we state guarantees in L^2 -Wasserstein distance \mathcal{W}^2 . The strong convexity assumption can be relaxed to asymptotic strong convexity — as in [5, 14, 8]. However, the resulting contraction rates, and in turn, asymptotic bias and complexity estimates will then depend on model and hyperparameters in a more intricate way. On the other hand, under global strong convexity, the dependence on model and hyperparameters is more transparent, and therefore, this setting has been a focus of much of the extant literature [12, 29, 36, 40] — as we briefly review below.

MSC 2010 subject classifications: Primary 60J05; secondary 65C05,65P10.

Keywords and phrases: MCMC, Hamiltonian Monte Carlo, Couplings.

1.1. *State of the Art.* At present, the Verlet time integrator is the method of choice for both unadjusted and adjusted HMC [7]. This is for sound reasons. Indeed, the Verlet integrator is cheap; like forward Euler it requires only one new gradient evaluation per integration step. The Verlet integrator also has the maximal stability interval for the simple harmonic model problem¹[2, 11]. These properties are quite relevant to uHMC [8]. Moreover, the geometric properties of the Verlet integrator (symplecticity and reversibility) are key to making the method Metropolis-adjustable [21, 7]. Unsurprisingly, most research work on HMC has been devoted to studying unadjusted/adjusted HMC with Verlet time integration.

Under the assumption that the potential U has Lipschitz Hessian the Verlet integrator is also second-order accurate. Absent this assumption – in the rough potential setting – the accuracy of the integrator drops to first order. In turn, this drop in accuracy reduces the efficiency of HMC as an MCMC method and it is natural then to ask whether using a different integration scheme can produce a more efficient MCMC method. The work of Lee, Song and Vempala [29], which suggests a collocation method for the Hamiltonian flow, answers in the affirmative. This collocation method relies on a choice of basis functions (usually polynomials up to a certain degree) to represent the exact Hamiltonian flow, and uses a nonlinear solver per transition step. General complexity guarantees are given for these collocation methods, and they specifically consider the special case of a basis of piecewise quadratic polynomials defined on a time grid of step size h . In this case, Lee, Song and Vempala prove that uHMC with collocation can in principle produce an ε -accurate approximation of the target μ in \mathcal{W}^2 distance using

$$(1) \quad O\left(\left(\frac{d}{K}\right)^{1/2} \left(\frac{L}{K}\right)^{7/4} \varepsilon^{-1} \log\left(\frac{d}{K^{1/2}} \frac{L}{K} \frac{1}{\varepsilon}\right)^+\right) \text{ gradient evaluations}$$

when initialized at the minimum of U and run with duration $T \propto K^{1/4}/L^{3/4}$ where $\log(\mathbf{a})^+ = \max(\log(\mathbf{a}), 0)$ for $\mathbf{a} > 0$. The ratio L/K is known as the *condition number* of the function U , and it satisfies $L/K \geq 1$. In each transition step of uHMC, h is chosen to satisfy $h^{-1} \propto LT^3(|v| + |\nabla U(x)|T)K^{1/2}(L/K)^{3/2}\varepsilon^{-1}$, where $x, v \in \mathbb{R}^d$ are respectively the initial position and velocity at the current transition step. See [29, Theorem 1.6] for a detailed statement. Remarkably, this complexity guarantee requires no further regularity beyond K -strong convexity and L -gradient Lipschitz-ness of U . In practice, because uHMC with collocation requires a nonlinear solve per transition step, its widespread use is currently limited.

For comparison, the corresponding complexity for uHMC with Verlet time integration is

$$(2) \quad O\left(\left(\frac{d}{K}\right)^{1/2} \left(\frac{L}{K}\right)^2 \varepsilon^{-1} \log\left(\frac{\mathcal{W}^2(\mu, \nu)}{\varepsilon}\right)^+\right) \text{ gradient evaluations}$$

when initialized from a distribution ν with finite second moment and run with time step size $h \propto (L/K)^{-3/2}d^{-1/2}\varepsilon$ and duration $T \propto L^{-1/2}$. See [3, Chapter 5] for detailed statements and proofs of (2); which is based on [8, Appendix A]. Note that uHMC with Verlet underperforms uHMC with collocation in terms of condition number dependence. This substandard performance is due to the above mentioned drop in accuracy of the Verlet scheme, since uHMC with Verlet then requires a small time step size in order to resolve the asymptotic bias.

In principle, adjusted HMC can filter out all of the asymptotic bias due to time discretization. One would therefore hope that the dependence of the complexity on the accuracy parameter ε is at most logarithmic with adjustment. This result has recently been demonstrated under higher regularity assumptions and some restrictions on the initial conditions;

¹More precisely, among palindromic splitting methods with a fixed computational budget of N evaluations of the potential force per step, the method with the longest stability interval is a concatenation of N Verlet steps [7, Section 4.5].

specifically, assuming U is strongly convex, gradient Lipschitz and Hessian Lipschitz, Chen, Dwivedi, Wainwright, and Yu use a clever conductance argument to prove that adjusted HMC with Verlet from a ‘warm’ start can achieve ε accuracy in total variation distance using $O(d^{11/12}(L/K)\log(1/\varepsilon)^+)$ gradient evaluations [12]. In the same setting, implementable starting distributions are also considered; specifically, from a ‘feasible’ start the dimension and condition number dependence become slightly worse. At present, it remains an open problem to prove such bounds in the rough target density case and to relax the warm/feasible start conditions.

For analogous MCMC algorithms based on underdamped Langevin dynamics (ULD), the Randomized Midpoint Method (RMM) of Shen and Lee demonstrates that randomized time integrators can achieve provably optimal performance in the rough target density case [40]. The RMM method is essentially a randomized time integrator for ULD. In particular, Shen and Lee prove that RMM can produce an ε -accurate approximation of the target in \mathcal{W}^2 using

$$(3) \quad O\left(\left(\frac{d}{K}\right)^{1/3} \left(\frac{L}{K}\right)^{7/6} \varepsilon^{-2/3} \left(\log\left(\frac{d^{1/2}}{K^{1/2}\varepsilon}\right)^+\right)^{4/3}\right) \text{ gradient evaluations}$$

when initialized at rest (i.e., with zero initial velocity) within $(d/K)^{1/2}$ of the minimizer of U and with mass L , friction parameter 2, and time step size $h \propto (K/d)^{1/3} L^{-1/6} \varepsilon^{2/3}$. The proof uses a perturbative approach that leverages contractivity of exact ULD [15, 16]. Ergodicity of the RMM chain and a 3/2-order of accuracy for the \mathcal{W}^2 -asymptotic bias was subsequently proven in [23]. Additionally, Cao, Lu, and Wang demonstrate the optimality of RMM among ULD based MCMC algorithms in the rough target density setting [10]. The paper also surveys the existing literature on information theoretic lower bounds for randomized time integrators for ODEs and SDEs, such as [26, 27, 17].

Another related work is the shifted ODE method for ULD due to Foster, Lyons and Oberhauser [22]. In the strongly convex and rough potential setting considered here, the *exact* shifted ODE method can in principle produce an ε -accurate approximation of the target distribution in \mathcal{W}^2 distance using $O(d^{1/3}\varepsilon^{-2/3}\log(1/\varepsilon)^+)$ gradient evaluations with better complexity guarantees under higher regularity assumptions. The shifted ODE method is inspired by rough path theory, in which SDEs are realized as instances of Controlled Differential Equations (CDE). In particular, the shifted ODE method is constructed by tuning a controlling path such that the Taylor expansion of the CDE solution has the same low order terms as ULD. In practice, the ODE they obtain cannot be exactly solved, and consequently, they propose two discretizations based on a third order Runge-Kutta method and a fourth order splitting method. Numerical results for the discretizations are promising. The challenge is that the discretizations are trickier to analyze than the exact shifted ODE method.

HMC and ULD are indeed analogous stochastic processes, and in general, one might hope that results for ULD extend to uHMC. Elaborating on this analogy, Monmarché considers a parameterized family of unadjusted algorithms that include as special cases uHMC and ULD based algorithms, and permits a simultaneous and unified analysis and comparison [36]. In the strongly convex and rough potential setting, dimension-free lower bounds on the convergence rates of the algorithms are provided. Specializing to the case where U is also Hessian-Lipschitz, and focusing only on the dimension d and accuracy ε dependence, Monmarché finds that both the ULD and uHMC can produce an ε -accurate approximation of the target in $O(d^{1/2}\varepsilon^{-1/2}\log(d/\varepsilon)^+)$ gradient evaluations. Moreover, in the Gaussian case, Monmarché notes the rate for ULD and uHMC with partial momentum refreshment improves from K/L to $(K/L)^{1/2}$ dependence.

Considering the strength of the connection between uHMC and ULD highlighted above, and the improved complexity guarantee (3) provided by the use of randomized integrators

for ULD, it is natural to ask: *Is it possible to construct a randomized time integrator for uHMC that confers a better complexity guarantee in the rough target density case?* Since Hamiltonian dynamics does not explicitly incorporate friction or diffusion like ULD does [33, 6], it is not obvious that this strategy yields a better complexity guarantee than uHMC with Verlet. At a technical level, understanding the contractivity and asymptotic bias of the uHMC algorithm requires developing new mathematical arguments to resolve the improvement due to time integrator randomization. This paper answers the above question in the affirmative by suggesting a simple randomized time integrator for uHMC and directly analyzing the contractivity and asymptotic bias of the resulting MCMC algorithm in \mathcal{W}^2 distance.

1.2. Short Summary of Main Results. We now outline our main contributions. As above, we consider a target distribution $\mu(dx) \propto e^{-U(x)}dx$ where $U: \mathbb{R}^d \rightarrow \mathbb{R}_{\geq 0}$ is continuously differentiable, K -strongly convex and L -gradient Lipschitz. Let $(q_t(x, v), p_t(x, v))$ denote the exact flow of the Hamiltonian dynamics

$$\frac{d}{dt}q_t = p_t, \quad \frac{d}{dt}p_t = -\nabla U(q_t), \quad (q_0, v_0) = (x, v).$$

The randomized time integrator we suggest for the Hamiltonian flow is a stratified Monte Carlo (sMC) time integrator. Let $h > 0$ be a time step size and $\{t_k := kh\}_{k \in \mathbb{N}_0}$ be an evenly spaced time grid. This grid partitions time into subintervals $\{[t_k, t_{k+1})\}_{k \in \mathbb{N}_0}$ termed ‘strata’. Let $(\mathcal{U}_i)_{i \in \mathbb{N}_0}$ be a sequence of independent random variables such that $\mathcal{U}_i \sim \text{Uniform}(t_i, t_{i+1})$. One step of the sMC time integrator from t_i to t_{i+1} is given by

$$(4) \quad \tilde{Q}_{t_{i+1}} = \tilde{Q}_{t_i} + h\tilde{P}_{t_i} + \frac{1}{2}h^2\tilde{F}_{t_i}, \quad \tilde{V}_{t_{i+1}} = \tilde{P}_{t_i} + h\tilde{F}_{t_i}, \quad (\tilde{Q}_0, \tilde{V}_0) = (x, v),$$

where $\tilde{F}_{t_i} = -\nabla U(\tilde{Q}_{t_i} + (\mathcal{U}_i - t_i)\tilde{P}_{t_i})$ is the potential force evaluated at the ‘random point’ $\tilde{Q}_{t_i} + (\mathcal{U}_i - t_i)\tilde{P}_{t_i}$.

One intuition behind this scheme is as follows. Like Verlet integration, the sMC integrator updates the position variable on the i -th stratum $[t_i, t_{i+1})$ by a constant force \tilde{F}_{t_i} . However, unlike Verlet integration, the update rule involves the force evaluated at a random temporal point \mathcal{U}_i sampled from the i -th stratum, rather than from the left endpoint t_i of the i -th stratum $[t_i, t_{i+1})$. Moreover, unlike Verlet integration, the sMC integrator updates the velocity variable on the i -th stratum $[t_i, t_{i+1})$ by the same constant force \tilde{F}_{t_i} . Thus, this scheme uses only one new gradient evaluation per sMC integration step. This scheme is probably the simplest randomized time integrator for the Hamiltonian dynamics, but it certainly is not the only strategy. For example, one could approximate the force over the i -th stratum as $-\nabla U(q_{\mathcal{U}_i}(\tilde{Q}_{t_i}, \tilde{P}_{t_i}))$. However, as the true dynamics are unknown, this is not implementable. Choosing instead to first approximate $q_{\mathcal{U}_i}(\tilde{Q}_{t_i}, \tilde{P}_{t_i})$ using the forward Euler method, and then using the force at the resulting ‘random point’ to approximate the dynamics for both position and velocity over the i -th stratum $[t_i, t_{i+1})$ results in the sMC method described above. Replacing Verlet integration in this way, we obtain the uHMC algorithm with complete momentum refreshment described in Algorithm 1.

The main result of this paper states that uHMC with sMC time integration can produce an ε -accurate approximation of the target distribution using

$$(5) \quad O\left(\left(\frac{d}{K}\right)^{1/3} \left(\frac{L}{K}\right)^{5/3} \varepsilon^{-2/3} \log\left(\frac{\mathcal{W}^2(\mu, \nu)}{\varepsilon}\right)^+\right) \text{ gradient evaluations}$$

when initialized from an arbitrary distribution ν with finite second moment and run with the hyperparameters specified below in (8). The proof of this complexity guarantee follows from two theorems, which we briefly outline.

Algorithm 1: uHMC Transition Step with sMC Time Integration

Input: Current state of the chain $X_0 \in \mathbb{R}^d$, duration $T > 0$ and time step size $h > 0$.

- 1 Sample ξ from $\mathcal{N}(0, I_d)$;
- 2 Initialize sMC time integrator $\tilde{Q}_0 = X_0$; $\tilde{V}_0 = \xi$; $t_0 = 0$; $n = \lfloor T/h \rfloor$;
- 3 **for** $i = 0$ **to** $i = n - 1$ **do**
- 4 Update time $t_{i+1} = t_i + h$;
- 5 Sample \mathcal{U}_i uniformly from (t_i, t_{i+1}) ;
- 6 Evaluate potential force $\tilde{F}_{t_i} = -\nabla U(\tilde{Q}_{t_i} + (\mathcal{U}_i - t_i)\tilde{P}_{t_i})$;
- 7 Update position $\tilde{Q}_{t_{i+1}} = \tilde{Q}_{t_i} + h\tilde{P}_{t_i} + \frac{1}{2}h^2\tilde{F}_{t_i}$;
- 8 Update velocity $\tilde{V}_{t_{i+1}} = \tilde{P}_{t_i} + h\tilde{F}_{t_i}$;
- 9 **end**

Output: Next state of the chain $X_1 = \tilde{Q}_{t_n}$.

Let $\tilde{\pi}$ denote the one-step transition kernel of uHMC with sMC time integration. Firstly, assuming that $LT^2 \leq 1/8$ and $h \leq T$, Theorem 6 uses a synchronous coupling to prove \mathcal{W}^2 -contractivity of $\tilde{\pi}$

$$(6) \quad \mathcal{W}^2(\nu\tilde{\pi}, \eta\tilde{\pi}) \leq e^{-c} \mathcal{W}^2(\nu, \eta) \quad \text{with } c = KT^2/6,$$

where ν, η are arbitrary probability measures on \mathbb{R}^d with finite second moment. The \mathcal{W}^2 -contraction coefficient e^{-c} is uniform in the time step size. The proof of Theorem 6 relies on Lemma 5, which states almost sure contractivity of two copies of the sMC time integrator starting with the same initial velocities and with synchronized random temporal sample points. The proof of Lemma 5 crucially relies on K -strong convexity of U and the co-coercivity property of ∇U ; see Remark 4 for details on the latter. The proof involves a careful balance of these competing effects at the random points where the force is evaluated. As a corollary, $\tilde{\pi}$ admits a unique invariant measure $\tilde{\mu}$, but in general, due to time discretization error $\tilde{\mu} \neq \mu$.

Secondly, we upper bound the \mathcal{W}^2 -asymptotic bias of $\tilde{\pi}$, which quantifies $\mathcal{W}^2(\mu, \tilde{\mu})$. To this end, let π denote the transition kernel of exact HMC, which uses the exact Hamiltonian flow per transition step and satisfies $\mu\pi = \mu$. Theorem 10 uses a synchronous coupling of $\tilde{\pi}$ and π to prove: for $LT^2 \leq 1/8$ and $h \leq T$,

$$(7) \quad \mathcal{W}^2(\mu, \tilde{\mu}) \leq 142d^{1/2}c^{-1}(L/K)^{1/2}L^{1/4}h^{3/2}.$$

Remarkably, this upper bound only requires the assumption that U is K -strongly convex and L -gradient Lipschitz. The proof of Theorem 10 rests on the proof of L^2 -accuracy of the sMC integration scheme given in Lemma 7.

To obtain the stated complexity guarantee, the hyperparameters are tuned as follows:

$$(8) \quad \text{duration } T \propto L^{-1/2}, \text{ time step } h \propto \left(\varepsilon d^{-1/2} c \left(\frac{L}{K} \right)^{-1/2} L^{-1/4} \right)^{2/3}, \text{ and steps } m \propto c^{-1} \log \left(\frac{\mathcal{W}^2(\mu, \nu)}{\varepsilon} \right)^+.$$

For clarity, numerical prefactors are suppressed here, but are fully worked out in Theorem 11 and Remark 12. With this choice of hyperparameters, the \mathcal{W}^2 -contraction rate in (6) reduces to $c \propto K/L$, and we find that

$$\begin{aligned} \mathcal{W}^2(\nu\tilde{\pi}^m, \mu) &\leq \mathcal{W}^2(\nu\tilde{\pi}^m, \tilde{\mu}) + \mathcal{W}^2(\tilde{\mu}, \mu) \\ &\stackrel{(6)}{\leq} e^{-cm} \mathcal{W}^2(\nu, \tilde{\mu}) + \mathcal{W}^2(\tilde{\mu}, \mu) \leq e^{-cm} \mathcal{W}^2(\nu, \mu) + 2\mathcal{W}^2(\tilde{\mu}, \mu) \stackrel{(7)}{\leq} \varepsilon. \end{aligned}$$

Since the total number of gradient evaluations is $m \times T/h$, we obtain the complexity guarantee given in (5).

1.3. *Organization of the Paper.* The rest of the paper is organized as follows. Section 2 contains a definition of the new uHMC algorithm with sMC time integration (Definition 1); the assumptions on U (Assumption 2); a theorem on L^2 -Wasserstein Contractivity (Theorem 6); a theorem on L^2 -Wasserstein Asymptotic Bias (Theorem 10); and a L^2 -Wasserstein Complexity Guarantee (Theorem 11). Section 3 contains detailed proofs. An Appendix is included on: (i) ‘adjustable’ randomized time integrators which can be directly incorporated into the proposal of Metropolis-adjusted HMC (see Appendix A); and (ii) duration randomization which has a similar effect as partial momentum refreshment (see Appendix B).

We conclude this introduction by remarking that randomized time integration might also be useful in conjunction with either time step or duration adaptivity to deal with multiscale features in the target distribution — as in [28, 25, 24].

Acknowledgements. We wish to acknowledge Persi Diaconis for his support and encouragement of this collaboration. We also acknowledge Bob Carpenter, Tore Kleppe, Pierre Monmarché, Stefan Oberdörster, and Lihan Wang for feedback on a previous version of this paper. N. Bou-Rabee has been supported by the National Science Foundation under Grant No. DMS-2111224. M. Marsden also acknowledges his advisors Persi Diaconis and Lexing Ying for their support.

2. uHMC with sMC time integration.

2.1. *Notation.* Let $\mathcal{P}(\mathbb{R}^d)$ denote the set of all probability measures on \mathbb{R}^d , and denote by $\mathcal{P}^p(\mathbb{R}^d)$ the subset of probability measures on \mathbb{R}^d with finite p -th moment. Denote the set of all couplings of $\nu, \eta \in \mathcal{P}(\mathbb{R}^d)$ by $\text{Couplings}(\nu, \eta)$. For $\nu, \eta \in \mathcal{P}^p(\mathbb{R}^d)$, define the L^p -Wasserstein distance by

$$\mathcal{W}^p(\nu, \eta) := \left(\inf \left\{ E[|X - Y|^p] : \text{Law}(X, Y) \in \text{Couplings}(\nu, \eta) \right\} \right)^{1/p}.$$

2.2. *Definition of the uHMC Algorithm with sMC time integration.* Unadjusted Hamiltonian Monte Carlo (uHMC) is an MCMC method for approximate sampling from a ‘target’ probability distribution on \mathbb{R}^d of the form

$$(9) \quad \mu(dx) = \mathcal{Z}^{-1} \exp(-U(x)) dx, \quad \mathcal{Z} = \int_{\mathbb{R}^d} \exp(-U(x)) dx,$$

where $U: \mathbb{R}^d \rightarrow \mathbb{R}_{\geq 0}$ is assumed to be a continuously differentiable function such that $\mathcal{Z} < \infty$. The function U is termed ‘potential energy’ and $-\nabla U$ is termed ‘potential force’ since it is a force derivable from a potential.

First we recall the standard uHMC algorithm with Verlet time integration and complete momentum refreshment. The standard algorithm generates a Markov chain on \mathbb{R}^d using: (i) a Verlet time integrator for the Hamiltonian flow corresponding to the unit mass Hamiltonian $H(x, v) = (1/2)|v|^2 + U(x)$; and (ii) an i.i.d. sequence of random initial velocities $(\xi^k)_{k \in \mathbb{N}_0} \stackrel{i.i.d.}{\sim} \mathcal{N}(0, I_d)$. We want to highlight that there are exactly two hyper-parameters that need to be specified in this algorithm: the duration $T > 0$ of the Hamiltonian flow and the time step size $h \geq 0$; and for simplicity of notation, we often assume $T/h \in \mathbb{Z}$ when $h > 0$, which implies that $h \leq T$. Let $\{t_i := ih\}_{i \in \mathbb{N}_0}$ be an evenly spaced time grid. This grid partitions time into subintervals $\{[t_i, t_{i+1}]\}_{i \in \mathbb{N}_0}$ termed ‘strata’. In the $(k+1)$ -th uHMC transition step, a Verlet time integration is performed with initial position given by the k -th step of the chain and initial velocity given by ξ^k . The $(k+1)$ -th state of the chain is then the final position computed by Verlet. Recall that Verlet approximates the Hamiltonian flow using: (i) a piecewise quadratic approximation of positions which can be interpolated by a quadratic function

of time on each stratum $[t_i, t_{i+1})$; and (ii) a deterministic trapezoidal quadrature rule of the time integral of the potential force over each stratum $[t_i, t_{i+1})$ to update the velocities.

However, since in uHMC we are almost exclusively interested in a stochastic notion of accuracy of the numerical time integration [8, Theorem 3.6], it is quite natural to instead use a randomized time integrator for the Hamiltonian flow. This paper suggests one such randomized integration strategy. The basic idea is to replace the trapezoidal quadrature rule used by Verlet in each stratum with Monte Carlo. This construction will substantially relax the regularity requirements on the target density. The resulting integration scheme is an instance of a stratified Monte Carlo (sMC) time integrator. To precisely define this variant of uHMC, in addition to the i.i.d. sequence of random initial velocities $(\xi^k)_{k \in \mathbb{N}_0}$, we define an independent sequence of sequences $(\mathcal{U}_i^k)_{i, k \in \mathbb{N}_0}$ whose terms are independent uniform random variables $\mathcal{U}_i^k \sim \text{Uniform}(t_i, t_{i+1})$. A key ingredient in the algorithm is the *sMC flow* $(\tilde{Q}_t^k(x, v), \tilde{P}_t^k(x, v))$ from $(x, v) \in \mathbb{R}^{2d}$ defined by

$$(10) \quad \frac{d}{dt} \tilde{Q}_t^k = \tilde{P}_t^k, \quad \frac{d}{dt} \tilde{P}_t^k = -\nabla U(\tilde{Q}_{[t]_h}^k + (\tau_t^k - [t]_h) \tilde{P}_{[t]_h}^k)$$

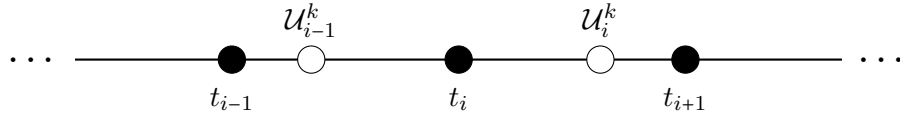
where we introduced the floor (resp. ceiling) function to the nearest time grid point less (resp. greater) than time t , i.e.,

$$(11) \quad [t]_h = \max\{s \in h\mathbb{Z} : s \leq t\}, \quad \lceil t \rceil_h = \min\{s \in h\mathbb{Z} : s \geq t\} \quad \text{for } h > 0,$$

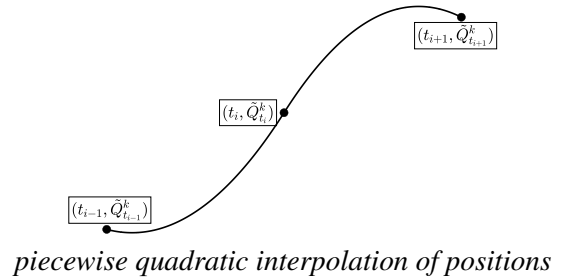
and the random temporal point in the i -th stratum

$$\tau_t^k = \mathcal{U}_i^k \quad \text{for } t \in [t_i, t_{i+1}),$$

as illustrated below.



By integrating (10), note that \tilde{Q}_t^k is a piecewise quadratic function of time that interpolates between the positions $\{\tilde{Q}_{t_i}^k\}$ and satisfies $\frac{d}{dt} \tilde{Q}_t^k = \tilde{P}_t^k$ and $\frac{d^2}{dt^2} \tilde{Q}_t^k \Big|_{t=t_i+} = -\nabla U(\tilde{Q}_{t_i}^k + (\mathcal{U}_i^k - t_i) \tilde{P}_{t_i}^k)$, while \tilde{P}_t^k is a piecewise linear function of time that interpolates between the velocities $\{\tilde{P}_{t_i}^k\}$.



For $h = 0$, we set $[t]_h = \lceil t \rceil_h = t$, drop the tildes in the notation, and since the corresponding flow is deterministic, we use lower case letters to denote the *exact flow* $(q_t(x, v), v_t(x, v))$ which satisfies

$$(12) \quad \frac{d}{dt} q_t = p_t, \quad \frac{d}{dt} p_t = -\nabla U(q_t).$$

On the time grid, the sMC flow is an unbiased estimator of the *semi-exact flow* $(\bar{q}_t(x, v), \bar{p}_t(x, v))$ which satisfies

$$(13) \quad \frac{d}{dt} \bar{q}_t = \bar{p}_t, \quad \frac{d}{dt} \bar{p}_t = -\frac{1}{h} \int_{[t]_h}^{\lceil t \rceil_h + h} \nabla U(\bar{q}_{[s]_h} + (s - [s]_h) \bar{p}_{[s]_h}) ds.$$

The semi-exact flow plays a key role in §2.5 to quantify the L^2 -accuracy of the sMC flow, and is itself somewhat related to the Average Vector Field method [38].

With this notation, the chain $(\tilde{X}^k)_{k \in \mathbb{N}_0}$ corresponding to uHMC with sMC time integration is defined as follows.

DEFINITION 1 (uHMC with sMC time integration). Given an initial state $x \in \mathbb{R}^d$, a duration hyperparameter $T > 0$, and time step size hyperparameter $h \geq 0$ with $T/h \in \mathbb{Z}$ for $h > 0$, define $\tilde{X}^0(x) := x$ and

$$\tilde{X}^{k+1}(x) := \tilde{Q}_T^k(\tilde{X}^k(x), \xi^k) \quad \text{for } k \in \mathbb{N}_0.$$

Let $\tilde{\pi}(x, A) = P[\tilde{X}^1(x) \in A]$ denote the corresponding one-step transition kernel.

For $h = 0$, we recover *exact HMC*. In this case, we drop all tildes in the notation, i.e., the k -th transition step is denoted by $X^k(x)$, and the corresponding transition kernel is denoted by π . The target measure μ is invariant under π , because the exact flow preserves the Boltzmann-Gibbs probability measure on \mathbb{R}^{2d} with density proportional to $\exp(-H(x, v))$, and μ is the first marginal of this measure. When $h > 0$, and under certain conditions (detailed below), $\tilde{\pi}$ has a unique invariant probability measure denoted by $\tilde{\mu}$, which typically approaches μ as $h \searrow 0$. In the sequel, and for the sake of brevity, uHMC refers to *uHMC with sMC time integration*.

In Appendix A, we detail a novel adjustable HMC algorithm that employs randomized time integration to approximate the exact Hamiltonian flow. Extending the sMC time integrator to be Metropolis-adjustable (see Definition 17) is a challenging task. Our approach involves constructing a randomized time integrator by randomly selecting from a parametric family of time integrators, each of which is reversible and volume-preserving. Remarkably the accept/reject rule for the adjustable randomized time integrator, similar to that in standard HMC, depends solely on the change in energy incurred along a composition of these randomly selected reversible and volume-preserving integrators. This result is particularly surprising given that the composition of reversible integrators is not necessarily reversible, whereas standard HMC requires a reversible proposal move (see, e.g., Section 5.3 of [7]). To clarify this surprising result, we provide a detailed but concise explanation in Appendix A.

2.3. Assumptions. To prove our main results, we assume the following.

ASSUMPTION 2. The potential energy function $U : \mathbb{R}^d \rightarrow \mathbb{R}$ is continuously differentiable and satisfies:

A.1 U has a global minimum at 0 and $U(0) = 0$.

A.2 U is L -gradient Lipschitz continuous, i.e., there exists $L > 0$ such that

$$|\nabla U(x) - \nabla U(y)| \leq L|x - y| \quad \text{for all } x, y \in \mathbb{R}^d.$$

A.3 U is K -strongly convex, i.e., there exists $K > 0$ such that

$$(\nabla U(x) - \nabla U(y)) \cdot (x - y) \geq K|x - y|^2 \quad \text{for all } x, y \in \mathbb{R}^d.$$

Assumptions **A.1-A.3** imply \mathcal{W}^2 -contractivity of the transition kernel of uHMC; see Theorem 6 below. By the Banach fixed point theorem, contractivity implies existence of a unique invariant probability measure of $\tilde{\pi}$ [3, Theorem 2.9]. The \mathcal{W}^2 -asymptotic bias of this invariant measure is upper bounded in Theorem 10.

REMARK 3. Under [A.1-A.3](#), using a quadratic Foster-Lyapunov function argument², it can be shown that the target distribution satisfies

$$\int_{\mathbb{R}^d} |x| \mu(dx) \leq \left(\int_{\mathbb{R}^d} |x|^2 \mu(dx) \right)^{1/2} \leq \left(\frac{d}{K} \right)^{1/2}$$

where in the first step we used Jensen's inequality. The bound is sharp in the sense that it is attained by a centered Gaussian random variable ξ with $E|\xi|^2 = d/K$.

REMARK 4. If U is continuously differentiable, convex, and L -gradient Lipschitz, then ∇U satisfies the following 'co-coercivity' property

$$(14) \quad |\nabla U(x) - \nabla U(y)|^2 \leq L(\nabla U(x) - \nabla U(y)) \cdot (x - y), \quad \text{for all } x, y \in \mathbb{R}^d.$$

This property plays a crucial role in proving a sharp \mathcal{W}^2 -contraction coefficient for the uHMC transition kernel in the globally strongly convex setting.

2.4. L^2 -Wasserstein Contractivity. Let $(\tilde{Q}_t(x, v), \tilde{P}_t(x, v))$ be a single realization of the SMC flow satisfying (10) from the initial condition $(x, v) \in \mathbb{R}^{2d}$ with a random sequence of independent temporal sample points $(\mathcal{U}_i)_{i \in \mathbb{N}_0}$ such that $\mathcal{U}_i \sim \text{Uniform}(t_i, t_{i+1})$. When U is K -strongly convex and L -gradient Lipschitz, the exact flow from different initial positions but synchronous initial velocities is itself contractive if $LT^2 \leq 1/4$ [13, Lemma 6].³ Analogously, if $LT^2 \leq 1/8$ and the time step size additionally satisfies $h \leq T$, the following lemma states that $|\tilde{Q}_T(x, v) - \tilde{Q}_T(y, v)|^2$ is almost surely contractive.

LEMMA 5 (Almost Sure Contractivity of SMC Time Integrator). Suppose that [A.1-A.3](#) hold. Let $T > 0$ satisfy:

$$(15) \quad LT^2 \leq 1/8,$$

and $h \geq 0$ satisfy $T/h \in \mathbb{Z}$ if $h > 0$. Then for all $x, y, v \in \mathbb{R}^d$,

$$(16) \quad |\tilde{Q}_T(x, v) - \tilde{Q}_T(y, v)|^2 \leq (1 - KT^2/3) |x - y|^2 \quad \text{almost surely}.$$

The proof of Lemma 5 is deferred to Section 3.1. By synchronously coupling both the random initial velocities and the random temporal sample points in two copies of uHMC starting at different initial conditions, and applying Lemma 5, we obtain the following.

THEOREM 6 (\mathcal{W}^2 -Contractivity of uHMC). Suppose that [A.1-A.3](#) hold. Let $T > 0$ and $h \geq 0$ be such that (15) holds with $T/h \in \mathbb{Z}$ if $h > 0$. Then for any pair of probability measures $\nu, \eta \in \mathcal{P}^2(\mathbb{R}^d)$,

$$(17) \quad \mathcal{W}^2(\nu \tilde{\pi}^m, \eta \tilde{\pi}^m) \leq (1 - c)^m \mathcal{W}^2(\nu, \eta) \quad \text{where}$$

$$(18) \quad c = KT^2/6.$$

PROOF. Let ω be an arbitrary coupling of $\nu, \eta \in \mathcal{P}^2(\mathbb{R}^d)$. By the coupling characterization of the \mathcal{W}^2 -distance,

$$\begin{aligned} \mathcal{W}^2(\nu \tilde{\pi}, \eta \tilde{\pi})^2 &\leq E_{(X, Y) \sim \omega, \xi \sim \mathcal{N}(0, I_d)} |\tilde{Q}_T(X, \xi) - \tilde{Q}_T(Y, \xi)|^2 \\ &\stackrel{\text{Lem. 5}}{\leq} (1 - KT^2/3) E_{(X, Y) \sim \omega} |X - Y|^2. \end{aligned}$$

²See Proposition 1(ii) of [20].

³Under $LT^2 \leq \min(1/4, K/L)$, Mangoubi and Smith first obtained a similar result [32].

Taking the infimum over all couplings ω and using the inequality $\sqrt{1-a} \leq 1 - a/2$ for $a \in [0, 1)$, we obtain the required result for $m = 1$. By iterating this inequality, the result extends to all $m \in \mathbb{N}$. \square

Note that the \mathcal{W}^2 -contraction coefficient in Theorem 6 is uniform in the time step size, and as $h \searrow 0$, recovers (up to a numerical prefactor) the sharp \mathcal{W}^2 -contraction coefficient of exact HMC [13, Lemma 6].

2.5. L^2 -Wasserstein Asymptotic Bias. As emphasized in previous works [8, 19], an apt notion of accuracy of the underlying time integrator in unadjusted HMC (and other inexact MCMC methods) is a stochastic one, e.g., L^2 -accuracy. Remarkably, the sMC time integrator is 3/2-order L^2 -accurate without higher regularity assumptions such as Lipschitz continuity of the Hessian of U .

LEMMA 7 (L^2 -accuracy of sMC Time Integrator). *Suppose that A.1-A.2 hold. Let $T > 0$ satisfy $LT^2 \leq 1/8$, and let $h > 0$ satisfy $T/h \in \mathbb{Z}$. Then for any $x \in \mathbb{R}^d$ and $k \in \mathbb{N}_0$ such that $t_k \leq T$,*

$$(19) \quad \left(E \left[|\tilde{Q}_{t_k}(x, v) - q_{t_k}(x, v)|^2 \right] \right)^{1/2} \leq 71 (|v| + \sqrt{L}|x|) L^{1/4} h^{3/2}.$$

Note that A.3 is not assumed in Lemma 19. The 3/2-order of L^2 -accuracy of the sMC time integrator is numerically verified in Figure 1.

PROOF OF LEMMA 7. The proof of L^2 -accuracy of the sMC integrator is carried out in two steps. In Lemma 14, we compare the sMC flow to the semi-exact flow. In Lemma 15, we compare the semi-exact flow to the exact flow. Using the triangle inequality and the bound $L^{1/4}h^{1/2} \leq 1/\sqrt{2}$, we obtain the required result with the numerical prefactor derived from summing the prefactors in (32) and (33) as follows:

$$\sqrt{2}e^{31/8} + 2e^{5/8}L^{1/4}h^{1/2} \leq \sqrt{2}(e^{31/8} + e^{5/8}) \leq 71.$$

\square

REMARK 8. *For comparison, under only the assumption that U is L -gradient Lipschitz, the order of accuracy of Verlet integration often drops from second to first order [8, Theorem 8]. This drop in accuracy is due to the use of a trapezoidal approximation of the integral of the force $-\nabla U$, and it is well known that the trapezoidal rule typically drops an order of accuracy if the integrand does not have a bounded second derivative. In turn, the accuracy of the integration scheme affects the asymptotic bias between the invariant measure of uHMC and the target distribution. Thus, a smaller time step size is needed to resolve the asymptotic bias of uHMC, which increases the complexity of the algorithm.*

REMARK 9. *The 3/2-order of L^2 -accuracy of the sMC time integrator is reminiscent of the classical Fundamental Theorem for L^2 -Convergence of Strong Numerical Methods for SDEs, which roughly states: if $p_1 \geq p_2 + 1/2$ and $p_2 > 1/2$ are the order of mean and mean-square accuracy (respectively), then the L^2 -accuracy of the method is of order $p_2 - 1/2$ [35, Theorem I.1.1]. For strong numerical methods for SDEs, this $(p_2 - 1/2)$ -order (as opposed to $(p_2 - 1)$ -order) is due to cancellations in the L^2 error expansion, due to independence of the Brownian increments. Consequently, the expectation of cross terms that involve the Brownian increments can vanish because they have zero mean. Here the cancellations (to leading order) occur because of independence of the sequence of random temporal sample*

points used by the *SMC* time integrator. Specifically, what happens is that the expectation of the random potential force appearing in the cross terms turns into an average of the force over the stratum, which confers higher accuracy in these cross-terms. Turning this heuristic into a rigorous proof relies on comparison to a semi-exact flow, which uses the mean force to update the position and velocity; see Lemmas 14 and 15 for details.

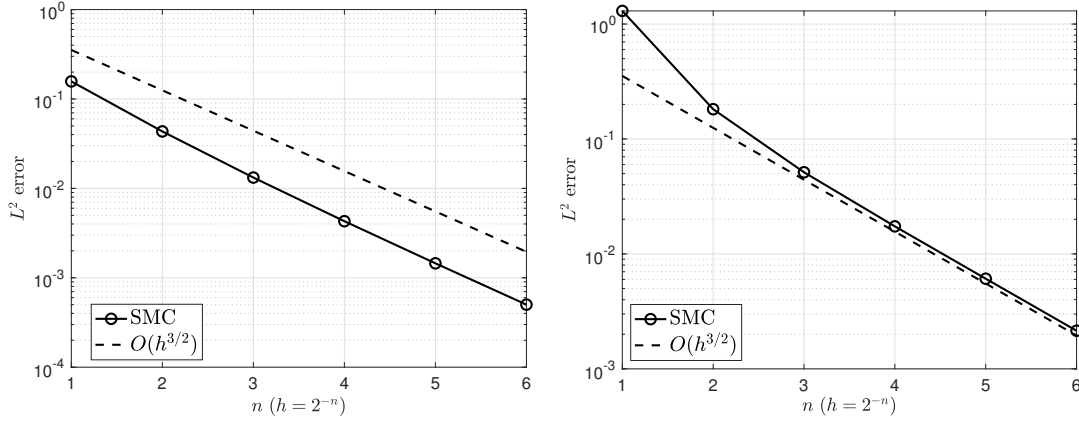


FIG 1. L^2 -Accuracy Verification. *Left Image:* A plot of the L^2 -error in (x, v) -space of the *SMC* time integrator for the linear oscillator with Hamiltonian $H(x, v) = (1/2)(v^2 + x^2)$. *Right Image:* A plot of the L^2 -error in (x, v) -space of the *SMC* time integrator for a double-well system with Hamiltonian $H(x, v) = (1/2)(v^2 + (1 - x^2)^2)$. Both simulations have initial condition $(2, 1)$ and unit duration. The time step sizes tested are 2^{-n} where n is given on the horizontal axis. The dashed curve is $2^{-3n/2} = h^{3/2}$ versus n .

Additionally, assuming A.3 holds, and using a triangle inequality trick [34, Remark 6.3], the L^2 -accuracy bound in Lemma 7 combined with the \mathcal{W}^2 -Contractivity in Theorem 6 can be used to bound the \mathcal{W}^2 -asymptotic bias.

THEOREM 10 (\mathcal{W}^2 -Asymptotic Bias of uHMC). *Suppose that A.1-A.3 hold. Let $T > 0$ and $h \geq 0$ be such that (15) holds with $T/h \in \mathbb{Z}$ if $h > 0$. Additionally, assume $LT^2 \leq 1/8$. Then*

$$\mathcal{W}^2(\mu, \tilde{\mu}) \leq 142 d^{1/2} c^{-1} (L/K)^{1/2} L^{1/4} h^{3/2}.$$

PROOF. By the triangle inequality,

$$\begin{aligned} \mathcal{W}^2(\mu, \tilde{\mu}) &= \mathcal{W}^2(\mu\pi, \tilde{\mu}\tilde{\pi}) \leq \mathcal{W}^2(\mu\pi, \mu\tilde{\pi}) + \mathcal{W}^2(\mu\tilde{\pi}, \tilde{\mu}\tilde{\pi}) \\ (20) \quad &\stackrel{\text{Thm. 6}}{\leq} \mathcal{W}^2(\mu\pi, \mu\tilde{\pi}) + (1-c)\mathcal{W}^2(\mu, \tilde{\mu}) \implies \mathcal{W}^2(\mu, \tilde{\mu}) \leq c^{-1}\mathcal{W}^2(\mu\pi, \mu\tilde{\pi}). \end{aligned}$$

Employing now Lemma 7, Remark 3, and $L/K \geq 1$ gives

$$\begin{aligned} \mathcal{W}^2(\mu\pi, \mu\tilde{\pi})^2 &\stackrel{\text{Lem. 7}}{\leq} E_{X \sim \mu, \xi \sim \mathcal{N}(0, I_d)} [|\tilde{Q}_{t_k}(X, \xi) - q_{t_k}(X, \xi)|^2] \\ &\stackrel{\text{Rmk. 3}}{\leq} 2 \cdot 71^2 d \left(1 + \frac{L}{K}\right) L^{1/2} h^3 \leq 4 \cdot 71^2 d \frac{L}{K} L^{1/2} h^3. \end{aligned}$$

Inserting this result back into (20) gives the required bound. \square

2.6. L^2 -Wasserstein Complexity. In sum, Theorem 6 implies, for any $\nu \in \mathcal{P}^2(\mathbb{R}^d)$, $\mathcal{W}^2(\tilde{\mu}, \nu\tilde{\pi}^m) \leq e^{-cm}\mathcal{W}^2(\tilde{\mu}, \nu)$; and Theorem 10 implies $\mathcal{W}^2(\mu, \tilde{\mu}) \leq O(h^{3/2})$. Together these two results imply $\mathcal{W}^2(\mu, \nu\tilde{\pi}^m)$ can be made arbitrarily small by choosing h sufficiently small and m sufficiently large. This complexity argument is quite standard for inexact MCMC methods [19, 8], but we briefly summarize it here for completeness.

THEOREM 11 (\mathcal{W}^2 -Complexity of uHMC). *Suppose that A.1-A.3 hold. Let $T > 0$ and $h \geq 0$ be such that (15) holds with $T/h \in \mathbb{Z}$ if $h > 0$. Let $\nu \in \mathcal{P}^2(\mathbb{R}^d)$. Define $\Delta(m) := \mathcal{W}^2(\mu, \nu\tilde{\pi}^m)$, i.e., the L^2 -Wasserstein distance to the target measure μ after m steps of uHMC initialized at ν . For any $\varepsilon > 0$, suppose that $h \geq 0$ and $m \in \mathbb{N}$ satisfy*

$$m \geq m^* := c^{-1} \log(2\mathcal{W}^2(\mu, \nu)/\varepsilon)^+, \quad h \leq h^* := e^{-4} \left(\frac{c(\varepsilon/2)}{d^{1/2}(L/K)^{1/2}L^{1/4}} \right)^{2/3}.$$

Then $\Delta(m) \leq \varepsilon$.

PROOF. Let $m \geq m^*$ and $h \leq h^*$. By the triangle inequality,

$$\begin{aligned} \Delta(m) &\leq \mathcal{W}^2(\mu, \tilde{\mu}) + \mathcal{W}^2(\tilde{\mu}, \nu\tilde{\pi}^m) \stackrel{\text{Thm. 6}}{\leq} \mathcal{W}^2(\mu, \tilde{\mu}) + e^{-cm}\mathcal{W}^2(\tilde{\mu}, \nu) \\ &\leq 2\mathcal{W}^2(\mu, \tilde{\mu}) + e^{-cm}\mathcal{W}^2(\mu, \nu) \stackrel{\text{Thm. 10}}{\leq} e^6 d^{1/2} c^{-1} \left(\frac{L}{K} \right)^{1/2} L^{1/4} h^{3/2} + e^{-cm}\mathcal{W}^2(\mu, \nu). \end{aligned}$$

Since $m \geq m^*$ and $h \leq h^*$, the required result follows. \square

REMARK 12 (\mathcal{W}^2 -Complexity Guarantee). *For any accuracy $\varepsilon > 0$, Theorem 11 states that $m \geq m^*$ uHMC transition steps with $h \leq h^*$ guarantee that $\Delta(m) \leq \varepsilon$. To turn this into a complexity guarantee, we specify the duration, and in turn, estimate the corresponding number of gradient evaluations. In particular, if one chooses the duration T to saturate the condition $LT^2 \leq 1/8$ in (15), i.e., $T = (8L)^{-1/2}$, then the \mathcal{W}^2 -contraction coefficient reduces to $c = 48^{-1}K/L$. Since each uHMC transition step involves T/h gradient evaluations, the corresponding number of gradient evaluations is*

$$(m \text{ transition steps}) \times (T/h \text{ integration steps}) = 8^{7/6} \cdot 6^{5/3} \cdot e^4 \left(\frac{d}{K} \right)^{1/3} \left(\frac{L}{K} \right)^{5/3} \left(\frac{\varepsilon}{2} \right)^{-2/3} \log \left(\frac{2\mathcal{W}^2(\mu, \nu)}{\varepsilon} \right)^+,$$

where explicitly $m = 48L/K \log \left(\frac{2\mathcal{W}^2(\mu, \nu)}{\varepsilon} \right)^+$, $T = (8L)^{-1/2}$ and $h = K(\varepsilon/2)^{2/3}/(4 \cdot 6^{2/3}d^{1/3}e^4L^{7/6})$.

2.7. Duration Randomization. We have discussed the benefits of time integration randomization for uHMC with complete momentum refreshment. Motivated by Monmarché's findings [36], we explore corresponding results for uHMC with partial momentum refreshment. Since partial momentum refreshment eventually leads to a complete momentum refreshment after a random number of steps, we consider uHMC with duration randomization, as introduced in §6 of [6].

The duration-randomized uHMC process is an implementable pure jump process on phase space \mathbb{R}^{2d} , alternating between two types of jumps: (i) a single step of a randomized time integrator for the Hamiltonian flow; and (ii) a complete momentum refreshment. This algorithm uses two hyperparameters: the time step h and the mean duration λ^{-1} . The existence of an explicit generator for the process facilitates detailed analyses of contractivity and asymptotic bias.

In Appendix B, we analyze the complexity of the duration-randomized uHMC process in detail and highlight its improvements over the duration-fixed uHMC chain (see Remark 24).

The improvement in complexity due to duration randomization is analogous to that from time integration randomization, leading to a better \mathcal{W}^2 -asymptotic bias. For time integration randomization, this improvement arises from averaging over the random midpoint used per integration step (see Remark 9). For duration randomization, it stems from averaging over the random duration.

Theorem 21 states that the \mathcal{W}^2 -contraction rate of this randomized uHMC process on phase space is $\gamma = K\lambda^{-1}/10$. The proof relies on a synchronous coupling of two copies of the duration-randomized uHMC process. When well-tuned, the contraction rate becomes $\gamma \propto K^{1/2}(K/L)^{1/2}$. Although this rate appears better than the duration-fixed uHMC rate of $c \propto K/L$, the rates are essentially identical when viewed on the same infinitesimal time scale, i.e., $c/T \propto \gamma$.

To quantify the asymptotic bias, we couple the duration-randomized uHMC process with an ‘exact’ counterpart. This coupling, which is itself a jump process with generator \mathcal{A}^C defined in (70), admits a Foster-Lyapunov function ρ^2 given by a quadratic ‘distorted’ metric on phase space [1], defined in (62). Using Itô’s formula for jump processes the corresponding finite-time drift condition is used in Theorem 23 to quantify the \mathcal{W}^2 -asymptotic bias of the duration-randomized uHMC process. By optimally tuning the hyperparameters, an improvement in the complexity of the duration-randomized uHMC process is found (see Remark 24).

3. Proofs. In this section we provide the remaining ingredients needed to prove Theorem 6 and Theorem 10.

3.1. *Proof of L^2 -Wasserstein contractivity.* The following proof carefully adapts ideas from [8] and Lemma 6 of [13]. The main idea in the proof is to carefully balance two competing effects at the random temporal sample points where the potential force is evaluated: (i) strong convexity of U (A.3); and (ii) co-coercivity of ∇U (Remark 4).

PROOF OF LEMMA 5. Let $t \in [0, T]$. Introduce the shorthands

$$(21) \quad x_t := \tilde{Q}_{[t]_h}(x, v) + (\tau_t - [t]_h)\tilde{P}_{[t]_h}(x, v) \quad \& \quad y_t := \tilde{Q}_{[t]_h}(y, v) + (\tau_t - [t]_h)\tilde{P}_{[t]_h}(y, v),$$

where recall that $\tau_t = \mathcal{U}_i$ for $t \in [t_i, t_{i+1})$ and $(\mathcal{U}_i)_{i \in \mathbb{N}_0}$ is a sequence of independent random variables such that $\mathcal{U}_i \sim \text{Uniform}(t_i, t_{i+1})$. Let $z_t := x_t - y_t$,

$$Z_t := \tilde{Q}_t(x, v) - \tilde{Q}_t(y, v), \quad \text{and} \quad W_t := \tilde{P}_t(x, v) - \tilde{P}_t(y, v).$$

Let $A_t := |Z_t|^2$, $B_t := 2Z_t \cdot W_t$ and $a_t := |z_t|^2$. Our goal is to obtain an upper bound for A_t . To this end, define

$$\rho_t := \phi_t \cdot z_t, \quad \phi_t := \nabla U(x_t) - \nabla U(y_t),$$

and note that by A.2, A.3 and (14),

$$(22) \quad K a_t \stackrel{\text{A.3}}{\leq} \rho_t \stackrel{\text{A.2}}{\leq} L a_t, \quad |\phi_t|^2 \stackrel{(14)}{\leq} L \rho_t, \quad \text{for all } t \geq 0.$$

By (10), note that

$$(23) \quad \frac{d}{dt} Z_t = W_t, \quad \frac{d}{dt} W_t = -\phi_t.$$

As a consequence of (23), a short computation shows that A_t and B_t satisfy

$$(24) \quad \frac{d}{dt} A_t = B_t, \quad \frac{d}{dt} B_t = -K A_t + 2|W_t|^2 + \epsilon_t,$$

where $\epsilon_t := KA_t - 2Z_t \cdot \phi_t$. Introduce the shorthand notation

$$s_{t-r} := \frac{\sin(\sqrt{K}(t-r))}{\sqrt{K}}, \quad \text{and} \quad c_{t-r} := \cos(\sqrt{K}(t-r)),$$

which satisfy $c_{t-r} = -\frac{d}{dr}s_{t-r}$. By variation of parameters,

$$(25) \quad A_T = c_T A_0 + \int_0^T s_{T-r} (2|W_r|^2 + \epsilon_r) dr.$$

To upper bound the integral involving $|W_r|^2$ in (25), use (23) and note that $W_0 = 0$, since the initial velocities in the two copies are synchronized. Therefore,

$$(26) \quad |W_t|^2 = \left| \int_0^t \phi_s ds \right|^2 \leq t \int_0^t |\phi_s|^2 ds \leq Lt \int_0^t \rho_s ds$$

where in the second step we used Cauchy-Schwarz, and in the last step, we used (22). Note that since $LT^2 \leq 1/8$, s_{t-r} is monotonically decreasing with r ,

$$(27) \quad 0 \leq s_{t-r} \leq s_{t-s}, \quad \text{for } s \leq r \leq t \leq T \leq \frac{\pi/2}{\sqrt{K}}.$$

Therefore, combining (26) and (27), and by Fubini's Theorem,

$$\begin{aligned} \int_0^t s_{t-r} |W_r|^2 dr &\stackrel{(26)}{\leq} L \int_0^t \int_0^r r s_{t-r} \rho_s ds dr \stackrel{(27)}{\leq} L \int_0^t \int_0^r r s_{t-s} \rho_s ds dr \\ &\leq L \int_0^t \int_s^t r s_{t-s} \rho_s dr ds \leq (Lt^2/2) \int_0^t s_{t-s} \rho_s ds. \end{aligned}$$

In fact, as a byproduct of this calculation, observe that

$$(28) \quad \left(\int_0^t s_{t-r} |W_{[r]_h}|^2 dr \right) \vee \left(\int_0^t s_{t-r} |W_r|^2 dr \right) \leq (Lt^2/2) \int_0^t s_{t-s} \rho_s ds.$$

To upper bound the integral involving ϵ_r in (25), note by (23)

$$Z_t = Z_{[t]_h} + (t - [t]_h)W_{[t]_h} - \frac{(t - [t]_h)^2}{2} \phi_t,$$

and hence, $Z_t - z_t = (t - \tau_t)W_{[t]_h} - \frac{(t - [t]_h)^2}{2} \phi_t$ and

$$\begin{aligned} \epsilon_t &= KA_t - 2\rho_t - 2(Z_t - z_t) \cdot \phi_t = KA_t - 2\rho_t - 2(t - \tau_t)W_{[t]_h} \cdot \phi_t + (t - [t]_h)^2 |\phi_t|^2 \\ &= Ka_t - 2\rho_t - 2(t - \tau_t)W_{[t]_h} \cdot \phi_t + (t - [t]_h)^2 |\phi_t|^2 \\ &\quad + K \left| (t - \tau_t)W_{[t]_h} - \frac{(t - [t]_h)^2}{2} \phi_t \right|^2 + 2K \left((t - \tau_t)W_{[t]_h} - \frac{(t - [t]_h)^2}{2} \phi_t \right) \cdot z_t \\ &\stackrel{(22)}{\leq} Ka_t - 2\rho_t - 2(t - \tau_t)W_{[t]_h} \cdot \phi_t + (t - [t]_h)^2 |\phi_t|^2 \\ &\quad + K \left| (t - \tau_t)W_{[t]_h} - \frac{(t - [t]_h)^2}{2} \phi_t \right|^2 + 2K(t - \tau_t)W_{[t]_h} \cdot z_t \\ (29) \quad &\leq -2\rho_t + K(1 + Kh^2)a_t + (2h^2 + Kh^4/2)|\phi_t|^2 + 2(1 + Kh^2)|W_{[t]_h}|^2 \end{aligned}$$

where in the last step we used Cauchy-Schwarz and Young's product inequality; and in the next to last step we used that $z_t \cdot \phi_t = \rho_t \geq 0$, which follows from (22). Inserting these bounds

into the second term of (25) yields

$$\begin{aligned}
& \int_0^T s_{T-r} (2|W_r|^2 + \epsilon_r) dr \\
& \stackrel{(29)}{\leq} \int_0^T s_{T-r} (2|W_r|^2 + 2(1 + Kh^2)|W_{[r]_h}|^2 - 2\rho_r + (2h^2 + Kh^4/2)|\phi_r|^2 + K(1 + Kh^2)a_r) dr \\
& \stackrel{(28)}{\leq} \int_0^T s_{T-r} ([LT^2(2 + Kh^2) - 2]\rho_r + (2h^2 + Kh^4/2)|\phi_r|^2 + K(1 + Kh^2)a_r) dr \\
& \stackrel{(22)}{\leq} \int_0^T s_{T-r} ([Lh^2(2 + Kh^2/2) + LT^2(2 + Kh^2) - 2]\rho_r + K(1 + Kh^2)a_r) dr, \\
& \stackrel{(22)}{\leq} K \int_0^T s_{T-r} [Lh^2(2 + Kh^2/2) + LT^2(2 + Kh^2) - 2 + (1 + Kh^2)] a_r dr.
\end{aligned}$$

where in the last step we used that $K \leq L$, $h \leq T$, and $LT^2 \leq 1/8$. In fact, this upper bound is non-positive, and therefore, this term can be dropped from (25) to obtain $A_T \leq c_T A_0$. The required estimate is then obtained by inserting the elementary inequality

$$\begin{aligned}
c_T & \leq 1 - (1/2)KT^2 + (1/6)K^2T^4 \stackrel{(15)}{\leq} 1 - (1/2)KT^2 + (1/48)KT^2(K/L) \\
& \leq 1 - (1/2 - 1/48)KT^2
\end{aligned}$$

which is valid since $LT^2 \leq 1/8$ and $K \leq L$. The required result then holds because $1/2 - 1/48 = 23/48 > 1/3$. Note, the condition $LT^2 \leq 1/8$ was used twice in this proof to avoid complications due to potential periodicities in the underlying Hamiltonian flow. \square

3.2. A priori upper bounds for the Stratified Monte Carlo Integrator. The following a priori upper bounds for the sMC and semi-exact flows are useful to prove L^2 -accuracy of the sMC flow.

LEMMA 13 (A priori bounds). *Suppose A.1-A.2 hold. Let $T > 0$ satisfy $LT^2 \leq 1/8$ and let $h \geq 0$ satisfy $T/h \in \mathbb{Z}$ if $h > 0$. For any $x, y, u, v \in \mathbb{R}^d$, we have almost surely*

$$(30) \quad \sup_{s \leq T} |\tilde{Q}_s(x, v)| \vee \sup_{s \leq T} |\bar{q}_s(x, v)| \leq (1 + L(T^2 + Th)) \max(|x|, |x + Tv|),$$

$$(31) \quad \sup_{s \leq T} |\tilde{P}_s(x, v)| \vee \sup_{s \leq T} |\bar{p}_s(x, v)| \leq |v| + LT(1 + L(T^2 + Th)) \max(|x|, |x + Tv|).$$

The proof of Lemma 13 is nearly identical to the proof of Lemma 3.1 of [5] and hence is omitted.

3.3. Proof of L^2 -Accuracy of sMC Integrator. The next two lemmas combined with the triangle inequality imply L^2 -accuracy of the sMC integrator given in Lemma 7.

LEMMA 14 (L^2 -accuracy of sMC Time Integrator with respect to Semi-Exact Flow). *Suppose A.1-A.2 hold. Let $T > 0$ satisfy $LT^2 \leq 1/8$ and let $h > 0$ satisfy $T/h \in \mathbb{Z}$. Then for any $x, v \in \mathbb{R}^d$ and $k \in \mathbb{N}_0$ such that $t_k \leq T$,*

$$(32) \quad \left(E[|\tilde{Q}_{t_k}(x, v) - \bar{q}_{t_k}(x, v)|^2] \right)^{1/2} \leq \sqrt{2} e^{31/8} L^{1/4} (|v| + L^{1/2}|x|) h^{3/2}.$$

For a heuristic explanation of the 3/2-order of accuracy appearing in (32), see Remark 9. As highlighted in the proof, this scaling results from the cancellations of $O(h)$ -terms due to the independence of the random temporal sample points used by the sMC time integrator.

LEMMA 15 (Accuracy of Semi-Exact Flow). *Suppose A.1-A.2 hold. Let $T > 0$ satisfy $LT^2 \leq 1/8$, and let $h > 0$ satisfy $T/h \in \mathbb{Z}$. Then for any $x, v \in \mathbb{R}^d$ and $k \in \mathbb{N}_0$ such that $t_k \leq T$,*

$$(33) \quad |\bar{q}_{t_k}(x, v) - q_{t_k}(x, v)| \leq 2e^{5/8} L^{1/2} (|v| + L^{1/2}|x|) h^2.$$

The proofs of these lemmas use a discrete Grönwall inequality, which we include here for the reader's convenience.

LEMMA 16 (Discrete Grönwall inequality). *Let $\lambda, h \in \mathbb{R}$ be such that $1 + \lambda h > 0$. Suppose that $(g_k)_{k \in \mathbb{N}_0}$ is a non-decreasing sequence, and $(a_k)_{k \in \mathbb{N}_0}$ satisfies $a_{k+1} \leq (1 + \lambda h)a_k + g_k$ for $k \in \mathbb{N}_0$. Then it holds*

$$a_k \leq (1 + \lambda h)^k a_0 + \frac{1}{\lambda h} ((1 + \lambda h)^k - 1) g_{k-1}, \quad \text{for all } k \in \mathbb{N}.$$

PROOF OF LEMMA 14. Let $(\tilde{Q}_t(x, v), \tilde{P}_t(x, v))$ be a realization of the sMC flow from the initial condition $(x, v) \in \mathbb{R}^{2d}$ which satisfies (10). A key ingredient in this proof are the a priori upper bounds in Lemma 13. In particular, since $L(T^2 + Th) \leq 1/4$, which follows from the hypotheses $LT^2 \leq 1/8$ and $T/h \in \mathbb{Z}$, (31) and the Cauchy-Schwarz inequality imply that

$$(34) \quad \sup_{s \leq T} |\tilde{P}_s(x, v)|^2 \vee \sup_{s \leq T} |\bar{p}_s(x, v)|^2 \leq 3|v|^2 + 4L^2 T^2 (|x|^2 + T^2 |v|^2).$$

For all $t \geq 0$, let \mathcal{F}_t denote the sigma-algebra of events up to t generated by the independent sequence of random temporal sample points $(\mathcal{U}_i)_{i \in \mathbb{N}_0}$. Define the distorted ℓ_2 -metric⁴

$$(35) \quad \rho_t^2 := E|Z_t|^2 + L^{-1/2} E\langle W_t, Z_t \rangle + L^{-1} E|W_t|^2,$$

where $Z_t := \tilde{Q}_t(x, v) - \bar{q}_t(x, v)$ and $W_t := \tilde{P}_t(x, v) - \bar{p}_t(x, v)$. By Young's product inequality,

$$(36) \quad \frac{1}{2} (E|Z_t|^2 + L^{-1} E|W_t|^2) \leq \rho_t^2 \leq \frac{3}{2} (E|Z_t|^2 + L^{-1} E|W_t|^2).$$

As a shorthand notation, for any $k \in \mathbb{N}_0$, let

$$\tilde{F}_{t_k} := -\nabla U(\tilde{Q}_{t_k} + (\mathcal{U}_k - t_k)\tilde{P}_{t_k}), \quad \text{and} \quad \bar{F}_{t_k} := -E[\nabla U(\bar{q}_{t_k} + (\mathcal{U}_k - t_k)\bar{p}_{t_k})].$$

Since the sMC and semi-exact flows satisfy (10) and (13) respectively,

$$(37) \quad Z_{t_{k+1}} = Z_{t_k} + hW_{t_k} + \frac{h^2}{2} (\tilde{F}_{t_k} - \bar{F}_{t_k}),$$

$$(38) \quad W_{t_{k+1}} = W_{t_k} + h(\tilde{F}_{t_k} - \bar{F}_{t_k}).$$

Using, in turn, the Cauchy-Schwarz inequality, the L -Lipschitz continuity of ∇U , and Jensen's inequality, we obtain:

$$(39) \quad \begin{aligned} E|\tilde{F}_{t_k} - \bar{F}_{t_k}|^2 &= E \left| \frac{1}{h} \int_{t_k}^{t_{k+1}} (\nabla U(\tilde{Q}_{t_k} + (\mathcal{U}_k - t_k)\tilde{P}_{t_k}) - \nabla U(\bar{q}_{t_k} + (u - t_k)\bar{p}_{t_k})) du \right|^2 \\ &\stackrel{\text{Cauchy-Schwarz}}{\leq} E \frac{1}{h} \int_{t_k}^{t_{k+1}} |\nabla U(\tilde{Q}_{t_k} + (\mathcal{U}_k - t_k)\tilde{P}_{t_k}) - \nabla U(\bar{q}_{t_k} + (u - t_k)\bar{p}_{t_k})|^2 du \\ &\stackrel{\text{A.2}}{\leq} \frac{L^2}{h} E \int_{t_k}^{t_{k+1}} |Z_{t_k} + (\mathcal{U}_k - t_k)\tilde{P}_{t_k} - (u - t_k)\bar{p}_{t_k}|^2 du \\ &\stackrel{\text{Jensen}}{\leq} 3L^2 E|Z_{t_k}|^2 + 3L^2 h^2 (E|\tilde{P}_{t_k}|^2 + |\bar{p}_{t_k}|^2). \end{aligned}$$

⁴This type of quadratic "distorted" metric naturally arises in the study of the large-time behavior of dynamical systems with a Hamiltonian part; e.g., see (2.51) of [1]. Here we use the distorted metric differently, namely to quantify L^2 -accuracy of the sMC time integrator.

Moreover, since the sMC flow is an unbiased estimator of the semi-exact flow, and due to independence of the random temporal sample points used by the sMC time integrator,

$$\begin{aligned} |E[\tilde{F}_{t_k} - \bar{F}_{t_k} | \mathcal{F}_{t_k}]| &= |E[\nabla U(\bar{q}_{t_k} + (\mathcal{U}_k - t_k)\bar{p}_{t_k}) - \nabla U(\tilde{Q}_{t_k} + (\mathcal{U}_k - t_k)\tilde{P}_{t_k}) | \mathcal{F}_{t_k}]|, \\ (40) \quad &\stackrel{\text{A.2}}{\leq} L|Z_{t_k}| + Lh|W_{t_k}|, \end{aligned}$$

and it follows that,

$$\begin{aligned} E\langle Z_{t_k}, \tilde{F}_{t_k} - \bar{F}_{t_k} \rangle &= E\langle Z_{t_k}, E[\tilde{F}_{t_k} - \bar{F}_{t_k} | \mathcal{F}_{t_k}] \rangle \leq E(|Z_{t_k}| \cdot |E[\tilde{F}_{t_k} - \bar{F}_{t_k} | \mathcal{F}_{t_k}]|) \\ &\stackrel{(40)}{\leq} LE[|Z_{t_k}|(|Z_{t_k}| + h|W_{t_k}|)] \\ (41) \quad &\leq (3/2)LE|Z_{t_k}|^2 + (1/2)Lh^2E|W_{t_k}|^2 \end{aligned}$$

where we used, in turn, the Cauchy-Schwarz inequality, (40), and Young's product inequality. Similarly,

$$(42) \quad E\langle W_{t_k}, \tilde{F}_{t_k} - \bar{F}_{t_k} \rangle \leq LE[|W_{t_k}|(|Z_{t_k}| + h|W_{t_k}|)]$$

$$(43) \quad \leq (1/2)Lh^{-1}E|Z_{t_k}|^2 + (3/2)LhE|W_{t_k}|^2.$$

By (37) and (38),

(44)

$$\begin{aligned} \rho_{t_{k+1}}^2 &= \text{I} + \text{II} + \text{III} \quad \text{where we have introduced} \\ \text{I} &:= E|Z_{t_k}|^2 + (L^{-1/2} + 2h)E\langle Z_{t_k}, W_{t_k} \rangle + (L^{-1} + L^{-1/2}h + h^2)E|W_{t_k}|^2, \\ \text{II} &:= (h^2 + L^{-1/2}h)E\langle Z_{t_k}, \tilde{F}_{t_k} - \bar{F}_{t_k} \rangle + h(h^2 + \frac{3}{2}L^{-1/2}h + 2L^{-1})E\langle W_{t_k}, \tilde{F}_{t_k} - \bar{F}_{t_k} \rangle, \\ \text{III} &:= (\frac{h^4}{4} + L^{-1/2}\frac{h^3}{2} + L^{-1}h^2)E|\tilde{F}_{t_k} - \bar{F}_{t_k}|^2. \end{aligned}$$

Since $Lh^2 \leq 1/8$ implies $L^{1/2}h \leq 1/2$,

$$\begin{aligned} \text{I} &\leq (1 + 2L^{1/2}h)\rho_{t_k}^2 + (L^{1/2}h + Lh^2 - 2L^{1/2}h)L^{-1}E|W_{t_k}|^2 \\ (45) \quad &\leq (1 + 2L^{1/2}h)\rho_{t_k}^2 + L^{1/2}h(1 + \frac{1}{2} - 2)L^{-1}E|W_{t_k}|^2 \leq (1 + 2L^{1/2}h)\rho_{t_k}^2. \end{aligned}$$

By (41), (42) and (43),

$$\begin{aligned} \text{II} &\leq (h^2 + L^{-1/2}h) \left(\frac{3}{2}LE|Z_{t_k}|^2 + \frac{1}{2}Lh^2E|W_{t_k}|^2 \right) \\ &\quad + (h^2 + \frac{3}{2}L^{-1/2}h) \left(\frac{1}{2}LE|Z_{t_k}|^2 + \frac{3}{2}Lh^2E|W_{t_k}|^2 \right) + 2hL^{-1}E\langle W_{t_k}, \tilde{F}_{t_k} - \bar{F}_{t_k} \rangle \\ &\stackrel{(42)}{\leq} (2Lh^2 + \frac{9}{4}L^{1/2}h)E|Z_{t_k}|^2 + (2(Lh^2)^2 + \frac{11}{4}(Lh^2)^{3/2})L^{-1}E|W_{t_k}|^2 \\ &\quad + 2hE[|W_{t_k}|(|Z_{t_k}| + h|W_{t_k}|)] \\ &\leq (2Lh^2 + \frac{9}{4}L^{1/2}h)E|Z_{t_k}|^2 + (2(Lh^2)^2 + \frac{11}{4}(Lh^2)^{3/2})L^{-1}E|W_{t_k}|^2 \\ &\quad + 2(Lh^2)L^{-1}E[|W_{t_k}|^2] + 2h \left(\frac{L^{1/2}}{2}E[|Z_{t_k}|^2] + \frac{1}{2L^{1/2}}E[|W_{t_k}|^2] \right) \end{aligned}$$

$$\begin{aligned}
&= \left(\frac{13}{4} + 2L^{1/2}h \right) L^{1/2}hE[|Z_{t_k}|^2] \\
&\quad + \left(2(Lh^2)^{3/2} + \frac{11}{4}Lh^2 + 2L^{1/2}h + 1 \right) (L^{1/2}h)L^{-1}E[|W_{t_k}|^2] \\
&\leq \left(\frac{13}{4} + 1 \right) L^{1/2}hE[|Z_{t_k}|^2] + \left(\frac{1}{8} + \frac{11}{32} + 2 \right) (L^{1/2}h)L^{-1}E[|W_{t_k}|^2] \\
(46) \quad &\leq \frac{17}{4}L^{1/2}h(E[|Z_{t_k}|^2] + L^{-1}E[|W_{t_k}|^2]) \stackrel{(36)}{\leq} \frac{17}{2}(L^{1/2}h)\rho_{t_k}^2
\end{aligned}$$

where we used $L^{1/2}h \leq 1/2$, $Lh^2 \leq 1/8$ and (36). Finally, by (39), and using once more $L^{1/2}h \leq 1/2$, $Lh^2 \leq 1/8$ and (36),

$$\begin{aligned}
\text{III} &\leq \left(\frac{h^4}{4} + L^{-1/2}\frac{h^3}{2} + L^{-1}h^2 \right) (3L^2E|Z_{t_k}|^2 + 3L^2h^2(E|\tilde{P}_{t_k}|^2 + |\bar{p}_{t_k}|^2)) \\
&\leq 2L^{1/2}hE|Z_{t_k}|^2 + \left(\frac{3}{4}(Lh^2)^2 + \frac{3}{2}(Lh^2)^{3/2} + 3Lh^2 \right) h^2(E|\tilde{P}_{t_k}|^2 + |\bar{p}_{t_k}|^2) \\
(47) \quad &\stackrel{(36)}{\leq} 4L^{1/2}h\rho_{t_k}^2 + \left(\frac{3}{4}(Lh^2)^2 + \frac{3}{2}(Lh^2)^{3/2} + 3Lh^2 \right) h^2(L|x|^2 + \frac{49}{8}|v|^2)
\end{aligned}$$

where in the last step we inserted the a priori upper bounds from (34). Inserting (45), (46) and (47) into (44) yields

$$\rho_{t_{k+1}}^2 \leq \left(1 + \frac{29}{2}L^{1/2}h \right) \rho_{t_k}^2 + \left(\frac{3}{4}(Lh^2)^2 + \frac{3}{2}(Lh^2)^{3/2} + 3Lh^2 \right) h^2(L|x|^2 + \frac{49}{8}|v|^2).$$

By discrete Grönwall inequality (Lemma 16),

$$\begin{aligned}
\rho_{t_k}^2 &\leq \frac{6}{29}e^{29L^{1/2}T/2} \left(\frac{1}{4}(Lh^2) + \frac{1}{2}(Lh^2)^{1/2} + 1 \right) (Lh^2)^{1/2}h^2(L|x|^2 + \frac{49}{8}|v|^2) \\
&\leq \left(\frac{6}{29} \right) \left(\frac{41}{32} \right) \left(\frac{49}{8} \right) e^{29/4} L^{1/2}h^3(L|x|^2 + |v|^2) \leq e^{31/4} L^{1/2}h^3(L|x|^2 + |v|^2).
\end{aligned}$$

Here we simplified via $LT^2 \leq 1/8$, $L^{1/2}T \leq 1/2$ and $T/h \in \mathbb{Z}$. Employing (36) gives the required upper bound. \square

PROOF OF LEMMA 15. Define the weighted ℓ_1 -metric

$$(48) \quad \rho_t := |z_t| + L^{-1/2}|w_t|,$$

where $z_t := \bar{q}_t(x, v) - q_t(x, v)$ and $w_t := \bar{p}_t(x, v) - p_t(x, v)$. As a shorthand, let $\bar{F}_{t_k} := -E[\nabla U(\bar{q}_{t_k} + (\mathcal{U}_k - t_k)\bar{p}_{t_k})]$ and $F_t := -\nabla U(q_t)$. Since the exact and semi-exact flows satisfy (12) and (13) respectively, we have

$$\begin{aligned}
z_{t_{k+1}} &= z_{t_k} + hw_{t_k} + \int_{t_k}^{t_{k+1}} \int_{t_k}^s [\bar{F}_{t_k} - F_r] dr ds, \\
w_{t_{k+1}} &= w_{t_k} + h\bar{F}_{t_k} - \int_{t_k}^{t_{k+1}} F_s ds.
\end{aligned}$$

By the triangle inequality,

$$(49) \quad |z_{t_{k+1}}| \leq |z_{t_k}| + h|w_{t_k}| + \int_{t_k}^{t_{k+1}} \int_{t_k}^s |\bar{F}_{t_k} - F_r| dr ds,$$

$$(50) \quad |w_{t_{k+1}}| \leq |w_{t_k}| + |h\bar{F}_{t_k} - \int_{t_k}^{t_{k+1}} F_s ds|.$$

By the triangle inequality and [A.2](#),

$$\begin{aligned}
|\bar{F}_{t_k} - F_r| &\leq |F_r - F_{t_k}| + |F_{t_k} - \bar{F}_{t_k}| = |\nabla U(q_r) - \nabla U(q_{t_k})| + |F_{t_k} - \bar{F}_{t_k}| \\
&\stackrel{\text{A.2}}{\leq} L \left| \int_{t_k}^r p_u du \right| + L(|z_{t_k}| + h \sup_{s \leq T} |\bar{p}_s|) \\
(51) \quad &\leq Lh \sup_{s \leq T} |p_s| + L(|z_{t_k}| + h \sup_{s \leq T} |\bar{p}_s|).
\end{aligned}$$

Moreover, since the semi-exact flow incorporates the average of the potential force over each stratum,

$$\begin{aligned}
(52) \quad |h\bar{F}_{t_k} - \int_{t_k}^{t_{k+1}} F_s ds| &\leq \left| \int_{t_k}^{t_{k+1}} \left[\nabla U(\bar{q}_{t_k} + (s-t_k)\bar{p}_{t_k}) - \nabla U(q_{t_k} + (s-t_k)p_{t_k} + \int_{t_k}^s (s-r)F_r dr) \right] ds \right| \\
&\stackrel{\text{A.2}}{\leq} L(h|z_{t_k}| + \frac{h^2}{2}|w_{t_k}| + \frac{h^3}{6} \sup_{s \leq T} |\nabla U(q_s)|) \\
(53) \quad &\stackrel{\text{A.2}}{\leq} L \left(h|z_{t_k}| + \frac{h^2}{2}|w_{t_k}| + \frac{h^3}{6}(L|x| + LT \sup_{s \leq T} |p_s|) \right),
\end{aligned}$$

where in the last step we used

$$\begin{aligned}
\sup_{s \leq T} |\nabla U(q_s)| &= \sup_{s \leq T} |\nabla U(x) + \nabla U(q_s) - \nabla U(x)| \\
&\stackrel{\text{A.1,A.2}}{\leq} L|x| + L \sup_{s \leq T} \left| \int_0^s p_u du \right| \leq L|x| + LT \sup_{s \leq T} |p_s|.
\end{aligned}$$

Inserting [\(51\)](#) and [\(53\)](#) into [\(49\)](#) and [\(50\)](#) respectively, yields

$$(54) \quad |z_{t_{k+1}}| \leq (1 + \frac{1}{2}Lh^2)|z_{t_k}| + h|w_{t_k}| + Lh^3(\sup_{s \leq T} |p_s| \vee \sup_{s \leq T} |\bar{p}_s|),$$

$$(55) \quad |w_{t_{k+1}}| \leq (1 + \frac{1}{2}Lh^2)|w_{t_k}| + Lh|z_{t_k}| + \frac{1}{6}L^2h^3(|x| + T \sup_{s \leq T} |p_s|).$$

Inserting [\(54\)](#) and [\(55\)](#) into [\(48\)](#) evaluated at $t = t_{k+1}$, and using $L^{1/2}h \leq 1/2$, gives

$$\rho_{t_{k+1}} \leq (1 + \frac{5}{4}L^{1/2}h)\rho_{t_k} + \frac{1}{6}(L^{1/2}h)^3|x| + (L^{1/2}h)^3(L^{-1/2} + \frac{1}{6}T)(\sup_{s \leq T} |p_s| \vee \sup_{s \leq T} |\bar{p}_s|).$$

By the discrete Grönwall's inequality ([Lemma 16](#)),

$$\begin{aligned}
\rho_{t_k} &\leq \frac{4}{5}e^{(5/4)L^{1/2}T} \left(\frac{1}{6}(L^{1/2}h)^2|x| + (L^{1/2}h)^2(L^{-1/2} + \frac{1}{6}T)(\sup_{s \leq T} |p_s| \vee \sup_{s \leq T} |\bar{p}_s|) \right) \\
&\leq \frac{4}{5}e^{5/8}L^{1/2}h^2 \left(\frac{1}{6}L^{1/2}|x| + (1 + \frac{1}{6}L^{1/2}T)(\sup_{s \leq T} |p_s| \vee \sup_{s \leq T} |\bar{p}_s|) \right) \\
&\leq \frac{4}{5}e^{5/8}L^{1/2}h^2 \left(\frac{1}{6}L^{1/2}|x| + \left(\frac{13}{12} \right) \left(\frac{5}{8}L^{1/2}|x| + \frac{37}{32}|v| \right) \right) \\
&\leq \frac{4}{5}e^{5/8}L^{1/2}h^2 \left(\frac{27}{32}L^{1/2}|x| + \frac{481}{384}|v| \right) \leq 2e^{5/8}L^{1/2}(L^{1/2}|x| + |v|)h^2,
\end{aligned}$$

which gives [\(33\)](#) — as required. Note that in the last two steps we inserted the *a priori* upper bound in [\(31\)](#) and applied the conditions $LT^2 \leq 1/8$ and $L^{1/2}h \leq 1/2$. \square

APPENDIX A: METROPOLIS-ADJUSTABLE RANDOMIZED TIME INTEGRATORS

Here we present Metropolis-adjustable randomized time integrators, which are ‘adjustable’ in the following sense.

DEFINITION 17. *Let $\mu_{BG} := \mu \otimes \mathcal{N}(0, I_d)$ be the Boltzmann-Gibbs distribution. A randomized time integrator with transition kernel $\tilde{\Pi}$ is adjustable if there exists a density g on \mathbb{R}^{4d} such that:*

$$\mu_{BG}(dq dv) \tilde{\Pi}(\mathcal{S}(q, v), \mathcal{S}(dq' dv')) = g((q, v), (q', v')) \mu_{BG}(dq' dv') \tilde{\Pi}((q', v'), dq dv)$$

where $\mathcal{S} : (q, v) \mapsto (q, -v)$ is the velocity flip map.

In particular, the transition kernel $\tilde{\Pi}$ of an adjustable randomized time integrator can be used as a proposal distribution in a generalized Metropolis-Hastings algorithm with target measure μ_{BG} and transition kernel

$$\Pi((q, v), (dq' dv')) = \alpha((q, v), (q', v')) \tilde{\Pi}((q, v), dq' dv') + r(q, v) \delta_{\mathcal{S}(q, v)}(dq' dv')$$

where $\alpha((q, v), (q', v')) := \min(1, g((q', v'), (q, v)))$. It is straightforward to verify that the corresponding Metropolis-adjusted kernel Π satisfies generalized detailed balance w.r.t. μ_{BG} , i.e.,

$$\mu_{BG}(dq dv) \Pi(\mathcal{S}(q, v), \mathcal{S}(dq' dv')) = \mu_{BG}(dq' dv') \Pi((q', v'), dq dv)$$

and hence, leaves μ_{BG} invariant. Since the exact Hamiltonian flow $\varphi_t(x, v) := (q_t(x, v), p_t(x, v))$ in (12) is \mathcal{S} -reversible (i.e., $\varphi_{-t} = \mathcal{S} \circ \varphi_t \circ \mathcal{S}$) [7], the corresponding transition kernel $\Pi_t((x, v), \cdot) := \delta_{\varphi_t(x, v)}$ satisfies generalized detailed balance w.r.t. μ_{BG} . A general class of adjustable randomized time integrators are provided by the following proposition.

PROPOSITION 18. *Let $\{\theta_i\}_{i \in \mathcal{I}}$ be an indexed family of time integrators for (12) with index set \mathcal{I} . Let ρ be a probability distribution over \mathcal{I} . For each $i \in \mathcal{I}$, suppose that θ_i is: (i) volume-preserving and (ii) \mathcal{S} -reversible. Define*

$$\theta_{u_N \dots u_1} \equiv \theta_{u_N} \circ \dots \circ \theta_{u_2} \circ \theta_{u_1}, \quad \text{where } u_j \in \mathcal{I} \text{ for each } j \in \{1, \dots, N\}.$$

Then the randomized time integrator with transition kernel

$$\tilde{\Pi}((q, v), \cdot) = \int_{\mathcal{I}^N} \delta_{\theta_{u_N \dots u_1}(q, v)} \prod_{i=1}^N \rho(du_i)$$

is adjustable with $g((q, v), (q', v')) = e^{-[H(q, v) - H(q', v')]}$.

The proof of this proposition is straightforward and therefore omitted. As an application of this proposition, here is a concrete, implementable example of an adjustable randomized time integrator.

EXAMPLE 19 (Adjustable Randomized Time Integrator). *Let $\mathcal{I} = [0, 1/2]$, $h > 0$ be a time step size, $b \in \mathcal{I}$, and $\theta_b : \mathbb{R}^{2d} \rightarrow \mathbb{R}^{2d}$ be the following 2-stage palindromic integrator*

$$(56) \quad \theta_b(q, v) := \varphi_{bh}^{(A)} \circ \varphi_{h/2}^{(B)} \circ \varphi_{(1-2b)h}^{(A)} \circ \varphi_{h/2}^{(B)} \circ \varphi_{bh}^{(A)}(q, v),$$

where $\varphi_t^{(A)}(x, v) := (x + tv, v)$, and $\varphi_t^{(B)}(x, v) := (x, v + tF(x))$.

More explicitly, the scheme can be written as

$$(x, v) \mapsto \left(x + hv + (1-b)\frac{h^2}{2}F_+ + b\frac{h^2}{2}F_-, v + \frac{h}{2}[F_+ + F_-] \right),$$

where $F_+ := F(x + bhv)$ and $F_- := F(x + (1-b)hv + (1-2b)\frac{h^2}{2}F_+)$.

In general, this adjustable randomized time integrator requires two potential force evaluations per integration step. However, for $b = 0$ and $b = 1/2$, the scheme reduces to the velocity and position Verlet schemes, respectively. In this example, the probability distribution ρ could be the uniform distribution over $\text{Uniform}(0, 1/2)$. Alternatively, in order to average over position and velocity Verlet, ρ could be $\text{Uniform}\{0, 1/2\}$.

ALGORITHM 1 (Adjusted HMC with Randomized Time Integrator). *Given # of integration steps $N \in \mathbb{N}$, a probability measure ρ on \mathcal{I} , and the current state $(Q_0^a, V_0^a) \in \mathbb{R}^{2d}$, the method outputs an updated state $(Q_1^a, V_1^a) \in \mathbb{R}^{2d}$ using:*

Step 1 Draw independently $\{\mathcal{U}_i\}_{i=1}^N \stackrel{i.i.d.}{\sim} \rho$, $\mathcal{V} \sim \text{Uniform}(0, 1)$, and $\xi \sim \mathcal{N}(0, I_d)$.

Step 2 Set

$$(Q_1^a, V_1^a) = \begin{cases} \theta_{\mathcal{U}_N \dots \mathcal{U}_1}(Q_0^a, \xi) & \text{if } \mathcal{V} \leq \exp(-[H(\theta_{\mathcal{U}_N \dots \mathcal{U}_1}(Q_0^a, \xi)) - H(Q_0^a, \xi)]^+), \\ \mathcal{S}(Q_0^a, \xi) & \text{otherwise.} \end{cases}$$

APPENDIX B: DURATION-RANDOMIZED UHMC WITH SMC TIME INTEGRATION

Here we consider a duration-randomized uHMC algorithm with complete velocity refreshment (or *randomized uHMC* for short). In order to avoid periodicities in the Hamiltonian steps of HMC, duration randomization was suggested by Mackenzie in 1989 [31]. There are a number of ways to incorporate duration randomization into uHMC [9, 37, 6, 7]. One overlooked way, which is perhaps the simplest to analyze, is the unadjusted Markov jump process on phase space introduced in [6, Section 6], as briefly recounted below.

Before describing this process, we note that duration randomization has a similar effect as partial velocity refreshment. Intuitively speaking, after a random number of non-randomized uHMC transition steps with partial velocity refreshment, a complete refreshment occurs. Therefore, the findings given below are expected to hold for uHMC with partial velocity refreshment. However, in comparison to randomized uHMC, the analysis of uHMC with partial velocity refreshment is a more demanding task if the bounds have to be realistic with respect to model/hyper parameters.

B.1. Definition of Randomized uHMC with SMC time integration. The randomized uHMC process is an implementable, inexact MCMC method defined on *phase space* \mathbb{R}^{2d} and aimed at the Boltzmann-Gibbs distribution

$$(57) \quad \mu_{BG} := \mu \otimes \mathcal{N}(0, I_d).$$

First, we define the infinitesimal generator of the randomized uHMC process; and then describe how a path of this process can be realized.

To define the infinitesimal generator, let $\mathcal{U} \sim \text{Uniform}(0, h)$ and $\xi \sim \mathcal{N}(0, I_d)$ be independent random variables. Denote by $\Theta_h(x, v, \mathcal{U})$ a single step of the SMC time integrator operated with time step size $h > 0$ and initial condition $(x, v) \in \mathbb{R}^{2d}$ where $\Theta_h : \mathbb{R}^{2d} \times (0, 1) \rightarrow \mathbb{R}^{2d}$ is the deterministic map defined by

$$(58) \quad \Theta_h : (x, v, u) \mapsto \left(x + hv + \frac{h^2}{2} F(x + uv), v + hF(x + uv) \right).$$

On functions $f : \mathbb{R}^{2d} \rightarrow \mathbb{R}^{2d}$, the infinitesimal generator of the randomized uHMC process is defined by

$$(59) \quad \tilde{\mathcal{G}}f(x, v) = h^{-1} E(f(\Theta_h(x, v, \mathcal{U})) - f(x, v)) + \lambda E(f(x, \xi) - f(x, v)),$$

where $\lambda > 0$ is the intensity of velocity randomizations and $h > 0$ is the step size. The operator $\tilde{\mathcal{G}}$ is the generator of a Markov jump process $(\tilde{Q}_t, \tilde{P}_t)_{t \geq 0}$ with jumps that result in either: (i) a step of the SMC time integrator Θ_h ; or (ii) a complete velocity refreshment $(x, v) \mapsto (x, \xi)$. Due to time-discretization error in the SMC steps, this process has an asymptotic bias. Since the number of jumps of the process over $[0, t]$ is a Poisson process with intensity $\lambda + h^{-1}$, the mean number of steps of Θ_h (and hence, gradient evaluations) over a time interval of length $t > 0$ is t/h .

The random jump times and embedded chain of the randomized uHMC process may be produced by iterating the following algorithm.

ALGORITHM (Randomized uHMC). *Given intensity $\lambda > 0$, step size $h > 0$, the current time T_0 , and the current state $(\tilde{Q}_{T_0}, \tilde{V}_{T_0}) \in \mathbb{R}^{2d}$, the method outputs an updated state $(\tilde{Q}_{T_1}, \tilde{V}_{T_1}) \in \mathbb{R}^{2d}$ at the random time T_1 using:*

Step 1 *Draw an exponential random variable ΔT with mean $h/(\lambda h + 1)$, and update time via $T_1 = T_0 + \Delta T$.*

Step 2 *Draw $\xi \sim \mathcal{N}(0, I_d)$, $\mathcal{U} \sim \text{Uniform}(0, h)$, $\mathcal{V} \sim \text{Uniform}(0, 1)$, and set*

$$(\tilde{Q}_{T_1}, \tilde{V}_{T_1}) = \begin{cases} (\tilde{Q}_{T_0}, \xi) & \mathcal{V} \leq \frac{\lambda h}{1 + \lambda h} \\ \Theta_h(\tilde{Q}_{T_0}, \tilde{V}_{T_0}, \mathcal{U}) & \text{otherwise.} \end{cases}$$

Note: the random variables ΔT , ξ , \mathcal{V} , and \mathcal{U} are mutually independent and independent of the state of the process.

Let $\{T_i\}_{i \in \mathbb{N}_0}$ and $\{(\tilde{Q}_{T_i}, \tilde{V}_{T_i})\}_{i \in \mathbb{N}_0}$ denote the sequence of random jump times and states obtained by iterating this algorithm respectively. The path of the randomized uHMC process is then given by

$$(Q_t, p_t) = (\tilde{Q}_{T_i}, \tilde{V}_{T_i}) \quad \text{for } t \in [T_i, T_{i+1}).$$

Moreover, for any $t > 0$, the time-average of an observable $f : \mathbb{R}^{2d} \rightarrow \mathbb{R}$ along this trajectory is given by:

$$\frac{1}{t} \int_0^t f(Q_s, p_s) ds = \frac{1}{t} \sum_{0 \leq i \leq \infty} f(Q_{T_i}, V_{T_i}) (t \wedge T_{i+1} - t \wedge T_i).$$

Let $\theta_h : \mathbb{R}^{2d} \times (0, 1) \rightarrow \mathbb{R}^{2d}$ denote the map that advances the exact solution of the Hamiltonian dynamics over a single time step of size $h > 0$, i.e.,

$$\theta_h : (x, v) \mapsto \left(x + hv + \int_0^h (h-s) F(q_s(x, v)), v + \int_0^h F(q_s(x, v)) ds \right).$$

In the asymptotic bias proof, we couple the randomized uHMC process to a corresponding exact process $(Q_t, p_t)_{t \geq 0}$ with generator defined by:

$$(60) \quad \begin{aligned} \mathcal{G}f(x, v) &= h^{-1} E(f(\theta_h(x, v)) - f(x, v)) \\ &\quad + \lambda E(f(x, \xi) - f(x, v)). \end{aligned}$$

A key property of the exact process is that it leaves infinitesimally invariant the Boltzmann-Gibbs distribution μ_{BG} , and under our regularity assumptions on the target measure μ , it can be verified that μ_{BG} is also the unique invariant measure of the exact process.

B.2. L^2 -Wasserstein Contractivity of Randomized uHMC. Let $(\tilde{p}_t)_{t \geq 0}$ denote the transition semigroup of the randomized uHMC process $((\tilde{Q}_t, \tilde{P}_t))_{t \geq 0}$. A key tool in the contraction proof is a coupling of two copies of the randomized uHMC process with generator defined by

$$(61) \quad \begin{aligned} \tilde{\mathcal{G}}^C f(y) &= h^{-1} E(f(\Theta_h(x, v, \mathcal{U}), \Theta_h(\tilde{x}, \tilde{v}, \mathcal{U})) - f(y)) \\ &\quad + \lambda E(f((x, \xi), (\tilde{x}, \xi)) - f(y)) \end{aligned}$$

where $y = ((x, v), (\tilde{x}, \tilde{v})) \in \mathbb{R}^{4d}$. This coupling proof parallels the coupling approach in Ref. [4] for the PDMP corresponding to duration-randomized *exact* HMC; another strategy to prove contractivity is based on hypocoercivity [30].

To measure the distance between the two copies we use a distorted metric:

$$(62) \quad \begin{aligned} \rho(y)^2 &:= \frac{1}{4}|z|^2 + \frac{\lambda^{-1}}{2}\langle z, w \rangle + \lambda^{-2}|w|^2 = (z \ w) \mathbf{A} \begin{pmatrix} z \\ w \end{pmatrix}, \quad \text{where} \\ y &= ((x, v), (\tilde{x}, \tilde{v})) \in \mathbb{R}^{4d}, \quad z := x - \tilde{x}, \quad w := v - \tilde{v}, \quad \mathbf{A} := \begin{bmatrix} \frac{1}{4}\mathbf{1}_d & \frac{\lambda^{-1}}{4}\mathbf{1}_d \\ \frac{\lambda^{-1}}{4}\mathbf{1}_d & \lambda^{-2}\mathbf{1}_d \end{bmatrix}. \end{aligned}$$

This distorted metric involves the “ qv trick” behind Foster-Lyapunov functions for (i) dissipative Hamiltonian systems with random impulses [39]; (ii) second-order Langevin processes [43, 33, 41, 1]; and (iii) exact randomized HMC [6]. This cross-term plays a crucial role since it captures the contractivity of the potential force. Using the Peter-Paul inequality with parameter δ , we can compare this distorted metric to a ‘straightened’ metric,

$$(63) \quad \rho(y)^2 \leq \left(\frac{1}{4} + \frac{\lambda^{-1}\delta}{4} \right) |z|^2 + \left(\lambda^{-2} + \frac{\lambda^{-1}}{4\delta} \right) |w|^2 \stackrel{\delta=3\lambda}{\leq} |z|^2 + \frac{13}{12} \lambda^{-2} |w|^2$$

$$(64) \quad \leq \max(K^{-1}, \frac{13}{12} \lambda^{-2}) (K|z|^2 + |w|^2).$$

Similarly, the distorted metric is equivalent to the standard Euclidean metric

$$(65) \quad \frac{1}{8} \min(1, 4\lambda^{-2}) (|z|^2 + |w|^2) \leq \rho(y)^2 \leq \max(1, \frac{13}{12} \lambda^{-2}) (|z|^2 + |w|^2).$$

By applying the generator $\tilde{\mathcal{G}}^C$ on this distorted metric, and using the co-coercivity property of ∇U (see Remark 4), we can prove the following.

LEMMA 20. *Suppose that Assumptions A.1-A.3 hold and $\lambda > 0$, $h > 0$ satisfy*

$$(66) \quad (L\lambda^{-2})^{1/2} \leq 12^{-1},$$

$$(67) \quad \lambda h \leq 1.$$

Then $\tilde{\mathcal{G}}^C$ satisfies the following infinitesimal contractivity result

$$(68) \quad \tilde{\mathcal{G}}^C \rho^2 \leq -\gamma \rho^2, \quad \text{where } \gamma := 10^{-1} \frac{K}{\lambda}.$$

The proof of Lemma 20 is deferred to Section B.4. As a consequence of Lemma 20, we can prove L^2 Wasserstein contractivity of the transition semigroup $(\tilde{p}_t)_{t \geq 0}$ of randomized uHMC.

THEOREM 21. *Suppose that Assumptions A.1-A.3 hold and $\lambda > 0$, $h > 0$ satisfy (66) and (67), respectively. Then for any pair of probability measures $\nu, \eta \in \mathcal{P}^2(\mathbb{R}^{2d})$, and for any $t \geq 0$,*

$$(69) \quad \mathcal{W}^2(\nu \tilde{p}_t, \eta \tilde{p}_t) \leq 3 \max(\lambda, \lambda^{-1}) e^{-\gamma t/2} \mathcal{W}^2(\nu, \eta).$$

PROOF OF THEOREM 21. Let $(Y_t)_{t \geq 0}$ denote the coupling process on \mathbb{R}^{4d} generated by $\tilde{\mathcal{G}}^C$ with initial distribution given by an optimal coupling of the initial distributions ν and η w.r.t. the distance \mathcal{W}^2 . As a consequence of Lemma 20, the process $t \mapsto e^{\gamma t} \rho(Y_t)^2$ is a non-negative supermartingale. Moreover, by using the equivalence to the standard Euclidean metric given in (65),

$$\begin{aligned} \mathcal{W}^2(\nu \tilde{p}_t, \eta \tilde{p}_t)^2 &\leq 8 \max(1, \frac{1}{4} \lambda^2) E[\rho(Y_t)^2] \stackrel{(68)}{\leq} 8 \max(1, \frac{1}{4} \lambda^2) e^{-\gamma t} E[\rho(Y_0)^2] \\ &\leq 8 \max(1, \frac{1}{4} \lambda^2) \max(1, \frac{13}{12} \lambda^{-2}) e^{-\gamma t} \mathcal{W}^2(\nu, \eta)^2 \\ &\leq 9 \max(\lambda^2, \lambda^{-2}) e^{-\gamma t} \mathcal{W}^2(\nu, \eta)^2. \end{aligned}$$

Taking square roots of both sides gives the required result. \square

B.3. L^2 -Wasserstein Asymptotic Bias of Randomized uHMC. As a consequence of Theorem 21, the randomized uHMC process admits a unique invariant measure denoted by $\tilde{\mu}_{BG}$. Here we quantify the L^2 -Wasserstein asymptotic bias, i.e., $\mathcal{W}^2(\mu_{BG}, \tilde{\mu}_{BG})$. A key tool in the asymptotic bias proof is a coupling of the unadjusted and exact processes with generator

$$(70) \quad \begin{aligned} \mathcal{A}^C f(y) &= h^{-1} E(f(\theta_h(x, v), \Theta_h(\tilde{x}, \tilde{v}, \mathcal{U})) - f(y)) \\ &\quad + \lambda E(f((x, \xi), (\tilde{x}, \xi)) - f(y)), \end{aligned}$$

where $y = ((x, v), (\tilde{x}, \tilde{v})) \in \mathbb{R}^{4d}$.

LEMMA 22. *Suppose that Assumptions A.1-A.3 hold and $\lambda > 0$ and $h > 0$ satisfy (66) and (67). Let γ be the contraction rate of randomized uHMC in (68). Then \mathcal{A}^C satisfies the following infinitesimal drift condition*

$$(71) \quad \mathcal{A}^C \rho(y)^2 \leq -\frac{\gamma}{2} \rho(y)^2 + \frac{1}{2} \left(1 + \frac{1}{K \lambda^{-2}}\right) (L^{3/2} h |x|^2 + |v|^2) L h^3,$$

for all $y = ((x, v), (\tilde{x}, \tilde{v})) \in \mathbb{R}^{4d}$.

The proof of Lemma 22 is deferred to Section B.4. Let $(p_t)_{t \geq 0}$ denote the transition semigroup of the exact process $((Q_t, p_t))_{t \geq 0}$. We are now in position to quantify the asymptotic bias of randomized uHMC with SMC time integration.

THEOREM 23. *Suppose that Assumptions A.1-A.3 hold and $\lambda > 0$ and $h > 0$ satisfy (66) and (67). Then*

$$(72) \quad \mathcal{W}^2(\mu, \tilde{\mu})^2 \leq 8 \gamma^{-1} \left(1 + \frac{\lambda^2}{K}\right) L (L^{3/2} K^{-1} h^4 d + h^3 d).$$

REMARK 24 (Why duration randomization?). *Since the number of jumps of the randomized uHMC process over $[0, t]$ is a Poisson process with intensity $\lambda + h^{-1}$, the mean number of steps of Θ_h (and hence, gradient evaluations) over a time interval of length t is t/h . Let*

ν be the initial distribution of the randomized uHMC process. We choose λ to saturate (66), i.e., $\lambda = 12L^{1/2}$. The contraction rate in (68) then becomes

$$\gamma = 120^{-1} K^{1/2} \left(\frac{K}{L} \right)^{1/2}.$$

According to Theorem 21, to obtain ε -accuracy in \mathcal{W}^2 w.r.t. $\tilde{\mu}$, t can be chosen such that

$$(73) \quad t = 240K^{-1/2} \left(\frac{L}{K} \right)^{1/2} \log \left(\frac{3 \max(12^{-1}L^{1/2}, 12L^{-1/2}) \mathcal{W}^2(\nu, \tilde{\mu}_{BG})}{\varepsilon} \right)^+.$$

However, since $\tilde{\mu}$ is inexact, to resolve the asymptotic bias to ε -accuracy in \mathcal{W}^2 , Theorem 23 indicates that it suffices to choose h such that

$$8 \cdot 120 \cdot 13 \cdot \left(Kd \left(\frac{L}{K} \right)^4 h^4 + K^{1/2} d \left(\frac{L}{K} \right)^{5/2} h^3 \right) \leq \varepsilon^2.$$

In other words, it suffices to choose h such that

$$(74) \quad h^{-1} \geq 2 \max \left((8 \cdot 195)^{1/4} K^{1/2} \left(\frac{d}{K} \right)^{1/4} \frac{L}{K} \varepsilon^{-1/2}, 2(390)^{1/3} K^{1/2} \left(\frac{d}{K} \right)^{1/3} \left(\frac{L}{K} \right)^{5/6} \varepsilon^{-2/3} \right).$$

Combining (73) and (74) gives an overall complexity of

$$(75) \quad \frac{t}{h} \propto \max \left(\left(\frac{d}{K} \right)^{1/4} \left(\frac{L}{K} \right)^{3/2} \varepsilon^{-1/2}, \left(\frac{d}{K} \right)^{1/3} \left(\frac{L}{K} \right)^{4/3} \varepsilon^{-2/3} \right) \times \log \left(\frac{\max(L^{1/2}, L^{-1/2}) \mathcal{W}^2(\nu, \tilde{\mu}_{BG})}{\varepsilon} \right)^+.$$

Note, this complexity guarantee has a better dependence on the condition number to the one obtained in Remark 12 for uHMC with fixed duration. Additionally, in the high condition number regime $L/K > (d/K)^{1/2} \varepsilon^{-1}$, the dependence on both the dimension and accuracy also improves.

PROOF OF THEOREM 23. Let $(Y_t)_{t \geq 0}$ be the coupling process generated by \mathcal{A}^C in (70) with initial condition $Y_0 = ((Q_0, V_0), (Q_0, \tilde{V}_0)) \sim \mu_{BG} \otimes \tilde{\mu}_{BG}$. Fix $t > 0$. Then by the coupling characterization of the L^2 -Wasserstein distance, and Itô's formula for jump processes applied to $t \mapsto e^{\gamma t/2} \rho(Y_t)^2$, we obtain

$$\begin{aligned} \mathcal{W}^2(\mu, \tilde{\mu})^2 &\leq E(|Q_0 - \tilde{Q}_0|^2) \leq \frac{16}{3} E \left(\frac{3}{16} |Q_0 - \tilde{Q}_0|^2 + \lambda^{-2} \left| V_0 - \tilde{V}_0 + \frac{\lambda}{4} (Q_0 - \tilde{Q}_0) \right|^2 \right) \\ &\leq \frac{16}{3} E \rho(Y_0)^2 = \frac{16}{3} E \rho(Y_t)^2 \\ &\leq \frac{16}{3} \left(e^{-\gamma t/2} E \rho(Y_0)^2 + \int_0^t e^{-\gamma(t-s)/2} \left(\frac{\gamma}{2} \rho(Y_s)^2 + \mathcal{A}^C \rho(Y_s)^2 \right) ds \right) \\ &\stackrel{\text{Lem. 22}}{\leq} 8e^{-\gamma t/2} E \rho(Y_0)^2 + 4 \left(1 + \frac{1}{K\lambda^{-2}} \right) L h^3 \int_0^t e^{-\gamma(t-s)/2} (L^{3/2} h E |Q_s|^2 + E |p_s|^2) ds. \end{aligned}$$

Since the exact process leaves μ_{BG} invariant, the integrand in this expression simplifies

$$\begin{aligned} \mathcal{W}^2(\mu, \tilde{\mu})^2 &\leq 8e^{-\gamma t/2} E \rho(Y_0)^2 + 4 \left(1 + \frac{1}{K\lambda^{-2}} \right) L h^3 (L^{3/2} h E |Q_0|^2 + d) \int_0^t e^{-\gamma(t-s)/2} ds \\ &\stackrel{\text{Rem. 3}}{\leq} 8\gamma^{-1} \left(1 + \frac{\lambda^2}{K} \right) \frac{L}{K} h^3 d (L^{3/2} h + K). \end{aligned}$$

Simplifying this expression gives (72). □

B.4. Proofs for Randomized uHMC.

PROOF OF LEMMA 20. Let $F_{\mathcal{U}} := F(x + \mathcal{U}v)$, $\tilde{F}_{\mathcal{U}} := F(\tilde{x} + \mathcal{U}\tilde{v})$, $Z_{\mathcal{U}} := z + \mathcal{U}w$, and $\Delta F_{\mathcal{U}} := F_{\mathcal{U}} - \tilde{F}_{\mathcal{U}}$. Note that by A.2, A.3 and (14),

$$(76) \quad K|Z_{\mathcal{U}}|^2 \stackrel{\text{A.3}}{\leq} -\langle Z_{\mathcal{U}}, \Delta F_{\mathcal{U}} \rangle \stackrel{\text{A.2}}{\leq} L|Z_{\mathcal{U}}|^2, \quad |\Delta F_{\mathcal{U}}|^2 \stackrel{(14)}{\leq} -L\langle Z_{\mathcal{U}}, \Delta F_{\mathcal{U}} \rangle.$$

The idea of this proof is to decompose $\tilde{\mathcal{G}}^C \rho(y)^2$ into two terms: a gain Γ_0 and loss Λ_0 , and use (76) and the hyperparameter assumptions, to obtain an overall gain.

To this end, evaluate (61) at $f(y) = \rho(y)^2$ to obtain,

$$\begin{aligned} \tilde{\mathcal{G}}^C \rho(y)^2 &= h^{-1} E(\rho(\Theta_h(x, v, \mathcal{U}), \Theta_h(\tilde{x}, \tilde{v}, \mathcal{U}))^2 - \rho(y)^2) \\ &\quad + \lambda E(\rho((x, \xi), (\tilde{x}, \xi))^2 - \rho(y)^2) \\ &= \lambda^{-1} \left(\frac{\lambda h}{4} + \frac{1}{2} \right) E\langle Z_{\mathcal{U}}, \Delta F_{\mathcal{U}} \rangle \\ &\quad + \lambda^{-1} \left(-\frac{1}{2} + \frac{\lambda h}{4} \right) |w|^2 + \lambda^{-1} E \left[\left(\frac{\lambda^2 h^2}{4} + \frac{3\lambda h}{4} + 2 - \lambda \mathcal{U} \left(\frac{\lambda h}{4} + \frac{1}{2} \right) \right) \lambda^{-1} \langle w, \Delta F_{\mathcal{U}} \rangle \right] \\ &\quad + \lambda^{-1} \left(\frac{\lambda^3 h^3}{16} + \frac{\lambda^2 h^2}{4} + \lambda h \right) \lambda^{-2} E|\Delta F_{\mathcal{U}}|^2 = \Gamma_0 + \Lambda_0 \quad \text{where} \end{aligned}$$

$$(77) \quad \Gamma_0 := \lambda^{-1} \left(\frac{\lambda h}{4} + \frac{1}{2} \right) E\langle Z_{\mathcal{U}}, \Delta F_{\mathcal{U}} \rangle - \lambda^{-1} \frac{1}{2} |w|^2$$

$$(78) \quad \Lambda_0 := \lambda^{-1} \left(\frac{\lambda^3 h^3}{16} + \frac{\lambda^2 h^2}{4} + \lambda h \right) \lambda^{-2} E|\Delta F_{\mathcal{U}}|^2 + \lambda^{-1} \left(\frac{\lambda h}{4} \right) |w|^2 \\ + \lambda^{-1} E \left[\left(\frac{\lambda^2 h^2}{4} + \frac{3\lambda h}{4} + 2 - \lambda \mathcal{U} \left(\frac{\lambda h}{4} + \frac{1}{2} \right) \right) \lambda^{-1} \langle w, \Delta F_{\mathcal{U}} \rangle \right].$$

Note that the term $\lambda^{-1} E \left[\lambda \mathcal{U} \left(\frac{\lambda h}{4} + \frac{1}{2} \right) \lambda^{-1} \langle w, \Delta F_{\mathcal{U}} \rangle \right]$ was added and subtracted in order to leverage the co-coercivity property of ∇U at $Z_{\mathcal{U}}$; see (76). By the Peter-Paul inequality with parameter $(L\lambda^{-2})^{1/2}$, $\lambda h \leq 1$, and (76),

$$\begin{aligned} \Lambda_0 &\leq \lambda^{-1} \left(\frac{\lambda^3 h^3}{16} + \frac{\lambda^2 h^2}{4} + \lambda h + \frac{1}{2(L\lambda^{-2})^{1/2}} \left(\frac{\lambda^2 h^2}{4} + \frac{3\lambda h}{4} + 2 \right) \right) \lambda^{-2} E|\Delta F_{\mathcal{U}}|^2 \\ &\quad + \lambda^{-1} \left(\frac{\lambda h}{4} + \frac{(L\lambda^{-2})^{1/2}}{2} \left(\frac{\lambda^2 h^2}{4} + \frac{3\lambda h}{4} + 2 \right) \right) |w|^2 \\ &\stackrel{(67)}{\leq} \lambda^{-1} \left(\frac{21}{16} + \frac{3}{2(L\lambda^{-2})^{1/2}} \right) \lambda^{-2} E|\Delta F_{\mathcal{U}}|^2 + \lambda^{-1} \left(\frac{1}{4} + \frac{3(L\lambda^{-2})^{1/2}}{2} \right) |w|^2 \\ &\stackrel{(76)}{\leq} -\lambda^{-1} \left(\frac{21L\lambda^{-2}}{16} + \frac{3(L\lambda^{-2})^{1/2}}{2} \right) E\langle Z_{\mathcal{U}}, \Delta F_{\mathcal{U}} \rangle + \lambda^{-1} \left(\frac{1}{4} + \frac{3(L\lambda^{-2})^{1/2}}{2} \right) |w|^2 \\ (79) \quad &\stackrel{(66)}{\leq} -\lambda^{-1} \left(\frac{21}{16 \cdot 12^2} + \frac{1}{8} \right) E\langle Z_{\mathcal{U}}, \Delta F_{\mathcal{U}} \rangle + \lambda^{-1} \frac{3}{8} |w|^2. \end{aligned}$$

Combining Γ_0 in (77) with the upper bound on Λ_0 in (79) yields an overall gain

$$\tilde{\mathcal{G}}^C \rho(y)^2 \leq -\frac{1}{8} \lambda^{-1} \left(-\frac{5}{2} E\langle Z_{\mathcal{U}}, \Delta F_{\mathcal{U}} \rangle + |w|^2 \right) \stackrel{(76)}{\leq} -\frac{1}{8} \lambda^{-1} \left(\frac{5}{2} K E|Z_{\mathcal{U}}|^2 + |w|^2 \right).$$

By the Peter-Paul inequality with parameter h and noting that $\mathcal{U} \sim \text{Uniform}(0, h)$,

$$\begin{aligned} \tilde{\mathcal{G}}^C \rho(y)^2 &\leq -\frac{1}{8} \lambda^{-1} \left(\frac{5}{2} K (|z|^2 + h \langle z, w \rangle + \frac{h^2}{3} |w|^2) + |w|^2 \right) \\ &\leq -\frac{1}{8} \lambda^{-1} \left(\frac{5}{4} K |z|^2 + \left(1 - \frac{5}{12} K h^2 \right) |w|^2 \right) \stackrel{(66)}{\leq} -\frac{1}{9} \lambda^{-1} (K |z|^2 + |w|^2), \end{aligned}$$

where in the last step we used $K \leq L$, $\lambda h \leq 1$ and $(L\lambda^{-2})^{1/2} \leq 12^{-1}$. Inserting (64) and simplifying yields the required infinitesimal contraction result, i.e.,

$$\tilde{\mathcal{G}}^C \rho(y)^2 \leq -\frac{1}{9} \lambda^{-1} \min\left(\frac{12}{13} \lambda^2, K\right) \rho(y)^2 \leq -\frac{1}{10} \min(\lambda, K\lambda^{-1}) \rho(y)^2 = -\frac{K}{10\lambda} \rho(y)^2,$$

since $K\lambda^{-2} \leq 12^{-1} < 1$ implies $K < \lambda^2$, and hence, $\min(\lambda, K\lambda^{-1}) = K\lambda^{-1}$. \square

PROOF OF LEMMA 22. Let $F_{\mathcal{U}} := F(x + \mathcal{U}v)$, $\tilde{F}_{\mathcal{U}} := F(\tilde{x} + \mathcal{U}\tilde{v})$, $Z_{\mathcal{U}} := z + \mathcal{U}w$, and $\Delta F_{\mathcal{U}} := F_{\mathcal{U}} - \tilde{F}_{\mathcal{U}}$. The idea of this proof is related to the proof of Lemma 20: we carefully decompose $\mathcal{A}^C \rho(y)^2$ into a gain Γ_0 , loss Λ , and also, a discretization error Δ , and use (76) and the hyperparameter assumptions, to obtain a gain from the contractivity of the underlying randomized uHMC process up to discretization error. This estimate results in an infinitesimal drift condition, as opposed to an infinitesimal contractivity result. The quantification of the discretization error is related to the L^2 -error estimates for the sMC time integrator developed in Lemma 7, though the semi-exact flow only implicitly appears below, since the proof involves a one step analysis.

As a preliminary step, we develop some estimates that are used to bound the discretization error. Recall that $(q_s(x, v), p_s(x, v))$ denotes the exact Hamiltonian flow. Since $Lh^2 \leq 12^{-2} \leq 1/4$ (by the hypotheses: $(L\lambda^{-2})^{1/2} \leq 1/12$ and $\lambda h \leq 1$), (31) and the Cauchy-Schwarz inequality imply that

$$(80) \quad \sup_{s \leq h} |p_s(x, v)|^2 \leq 3|v|^2 + 4L^2 h^2 (|x|^2 + h^2 |v|^2) \leq 4L^2 h^2 |x|^2 + \frac{31}{10} |v|^2.$$

As a shorthand, define

$$\begin{aligned} F_1 &:= \frac{2}{h^2} \int_0^h (h-s) F(q_s(x, v)) ds, \quad \Delta F_1 := \frac{2}{h^2} \int_0^h (h-s) [F(q_s(x, v)) - F_{\mathcal{U}}] ds, \\ F_2 &:= \frac{1}{h} \int_0^h F(q_s(x, v)) ds, \quad \text{and} \quad \Delta F_2 := \frac{1}{h} \int_0^h [F(q_s(x, v)) - F_{\mathcal{U}}] ds. \end{aligned}$$

Then by the Cauchy-Schwarz inequality

$$\begin{aligned} E|\Delta F_1|^2 &= E \left| \frac{2}{h^2} \int_0^h (h-s) [F(q_s) - F_{\mathcal{U}}] ds \right|^2 \leq \frac{4}{h^4} \frac{h^3}{3} \int_0^h E |F(q_s) - F_{\mathcal{U}}|^2 ds \\ &\stackrel{\text{A.2}}{\leq} \frac{4}{h^4} \frac{L^2 h^3}{3} \int_0^h E |q_s - x - \mathcal{U}v|^2 ds = \frac{4}{h^4} \frac{L^2 h^3}{3} \int_0^h E \left| \int_0^s v_r dr - \mathcal{U}v \right|^2 ds \\ &\leq \frac{4}{h^4} \frac{2L^2 h^3}{3} \left(\int_0^h \left| \int_0^s v_r dr \right|^2 ds + h^3 |v|^2 \right) \leq \frac{8L^2 h^2}{3} \left(\sup_{s \leq h} |p_s|^2 + |v|^2 \right) \\ (81) \quad &\stackrel{(80)}{\leq} \frac{8L^2 h^2}{3} \left(4L^2 h^2 |x|^2 + \frac{41}{10} |v|^2 \right) \end{aligned}$$

where in the next to last step we used Young's product inequality. Similarly,

$$\begin{aligned}
E|\Delta F_2|^2 &= E \left| \frac{1}{h} \int_0^h [F(q_s(x, v)) - F_{\mathcal{U}}] ds \right|^2 \leq h^{-1} E \int_0^h |F(q_s(x, v)) - F_{\mathcal{U}}|^2 ds \\
&\stackrel{\text{A.2}}{\leq} \frac{L^2}{h} \int_0^h E \left| \int_0^s v_r dr - \mathcal{U}v \right|^2 ds \leq \frac{2L^2}{h} \left(\int_0^h \left| \int_0^s v_r dr \right|^2 ds + h^3 |v|^2 \right) \\
(82) \quad &\leq 2L^2 h^2 \left(\sup_{s \leq h} |p_s|^2 + |v|^2 \right) \stackrel{(80)}{\leq} 2L^2 h^2 \left(4L^2 h^2 |x|^2 + \frac{41}{10} |v|^2 \right).
\end{aligned}$$

Combining (81) and (82) we obtain

$$(83) \quad E|\Delta F_1|^2 \vee E|\Delta F_2|^2 \leq \frac{8}{3} L^2 h^2 \left(4L^2 h^2 |x|^2 + \frac{41}{10} |v|^2 \right) \leq 11L^2 h^2 (L^2 h^2 |x|^2 + |v|^2).$$

In order to obtain a sharp error estimate for the sMC time integrator, the following upper bound is crucial

$$\begin{aligned}
|E\Delta F_2| &= \left| \frac{1}{h} E \int_0^h [F(q_s(x, v)) - F_{\mathcal{U}}] ds \right| = \left| \frac{1}{h} \int_0^h [F(q_s(x, v)) - F(x + sv)] ds \right| \\
&\stackrel{\text{A.2}}{\leq} \frac{L}{h} \int_0^h |q_s(x, v) - (x + sv)| ds \leq \frac{L}{h} \int_0^h \left| \int_0^s (s-r) F(q_r(x, v)) dr \right| ds \\
&\stackrel{\text{A.2}}{\leq} \frac{L}{h} \int_0^h \int_0^s (s-r) |F(q_r(x, v))| dr ds \leq \frac{L^2 h^2}{6} (|x| + h \sup_{s \leq h} |p_s|) \\
&\stackrel{(31)}{\leq} \frac{L^2 h^2}{6} (|x| + h[|v| + Lh(1 + Lh^2)](|x| + h|v|)) \stackrel{(66)}{\leq} \frac{L^2 h^2}{5} (|x| + h|v|).
\end{aligned}$$

Thus, by Cauchy-Schwarz inequality,

$$(84) \quad |E\Delta F_2|^2 \leq \frac{2L^4 h^4}{25} (|x|^2 + h^2 |v|^2) \stackrel{(66)}{\leq} \frac{L^3 h^4}{12} (L|x|^2 + |v|^2),$$

in the last step the numerical pre-factor was simplified by using $\lambda h \leq 1$ and $(L\lambda^{-2})^{1/2} \leq 12^{-1}$.

Evaluate (70) at $f(y) = \rho(y)^2$ and expand to obtain

$$\begin{aligned}
\mathcal{A}^C \rho(y)^2 &= h^{-1} E (\rho(\theta_h(x, v), \Theta_h(\tilde{x}, \tilde{v}, \mathcal{U}))^2 - \rho(y)^2) \\
&\quad + \lambda E (\rho((x, \xi), (\tilde{x}, \xi))^2 - \rho(y)^2) \\
&= \lambda^{-1} \frac{1}{2} E \langle z, F_2 - \tilde{F}_{\mathcal{U}} \rangle + \lambda^{-1} \frac{\lambda h}{4} E \langle z, F_1 - \tilde{F}_{\mathcal{U}} \rangle + \lambda^{-1} \left(-\frac{1}{2} + \frac{\lambda h}{4} \right) |w|^2 \\
&\quad + \lambda^{-1} E \left(\frac{\lambda^2 h^2}{4} + \frac{\lambda h}{4} \right) \lambda^{-1} E \langle w, F_1 - \tilde{F}_{\mathcal{U}} \rangle + \lambda^{-1} \left(\frac{\lambda h}{2} + 2 \right) \lambda^{-1} E \langle w, F_2 - \tilde{F}_{\mathcal{U}} \rangle \\
&\quad + \lambda^{-1} \left(\frac{\lambda^3 h^3}{16} \right) \lambda^{-2} E |F_1 - \tilde{F}_{\mathcal{U}}|^2 + \lambda^{-1} (\lambda h) \lambda^{-2} E |F_2 - \tilde{F}_{\mathcal{U}}|^2 \\
&\quad + \lambda^{-1} \left(\frac{\lambda^2 h^2}{4} \right) \lambda^{-2} E \langle F_1 - \tilde{F}_{\mathcal{U}}, F_2 - \tilde{F}_{\mathcal{U}} \rangle \\
&= \Gamma_0 + \Lambda_0 + \lambda^{-1} \frac{\lambda h}{4} E \langle z, \Delta F_1 \rangle + \lambda^{-1} \frac{1}{2} \langle z, E \Delta F_2 \rangle \\
&\quad + \lambda^{-1} \left(\frac{\lambda^2 h^2}{4} + \frac{\lambda h}{4} \right) E \langle w, \lambda^{-1} \Delta F_1 \rangle + \lambda^{-1} \left(\frac{\lambda h}{2} + 2 \right) \langle w, \lambda^{-1} E \Delta F_2 \rangle
\end{aligned}$$

$$\begin{aligned}
& + \lambda^{-1} \left(\frac{\lambda^3 h^3}{8} + \frac{\lambda^2 h^2}{4} \right) E \langle \lambda^{-1} \Delta F_1, \lambda^{-1} \Delta F_u \rangle \\
& + \lambda^{-1} \left(\frac{\lambda^2 h^2}{4} + 2\lambda h \right) E \langle \lambda^{-1} \Delta F_2, \lambda^{-1} \Delta F_u \rangle \\
& + \lambda^{-1} \left(\frac{\lambda^3 h^3}{16} \right) \lambda^{-2} E |\Delta F_1|^2 + \lambda^{-1} (\lambda h) \lambda^{-2} E |\Delta F_2|^2 \\
& + \lambda^{-1} \left(\frac{\lambda^2 h^2}{4} \right) E \langle \lambda^{-1} \Delta F_1, \lambda^{-1} \Delta F_2 \rangle,
\end{aligned}$$

where Γ_0 and Λ_0 are the loss and gain from $\tilde{\mathcal{G}}^C \rho(y)^2$ in (77) and (78), respectively. Now we decompose $\mathcal{A}^C \rho(y)^2$

$$(85) \quad \mathcal{A}^C \rho(y)^2 \leq \Gamma_0 + \Lambda + \Delta \quad \text{where}$$

$$(86) \quad \Lambda := \Lambda_0 + \lambda^{-1} \frac{K}{18} |z|^2 + \lambda^{-1} \frac{1}{18} |w|^2 + \lambda^{-1} \left(\frac{\lambda^3 h^3}{16} + \frac{\lambda^2 h^2}{4} + \lambda h \right) \lambda^{-2} E |\Delta F_u|^2,$$

$$\begin{aligned}
\Delta & := \lambda^{-1} \left(\frac{9}{4K\lambda^{-2}} + 36 \left(1 + \frac{\lambda h}{4} \right)^2 \right) \lambda^{-2} E |\Delta F_2|^2 \\
& + \lambda^{-1} \left(\frac{\lambda^3 h^3}{8} + \frac{\lambda^2 h^2}{4} + \frac{9\lambda^2 h^2}{16K\lambda^{-2}} + 36 \left(\frac{\lambda^2 h^2}{8} + \frac{\lambda h}{8} \right)^2 \right) \lambda^{-2} E |\Delta F_1|^2
\end{aligned}$$

$$(87) \quad + \lambda^{-1} \left(2\lambda h + \frac{\lambda^2 h^2}{4} \right) \lambda^{-2} E |\Delta F_2|^2.$$

Here the loss Λ in $\mathcal{A}^C \rho(y)^2$ was separated from the discretization error Δ by applying the Peter-Paul inequality to the four cross terms involving z or w (i.e., $E \langle z, \Delta F_1 \rangle$, $E \langle z, \Delta F_2 \rangle$, $E \langle w, \lambda^{-1} \Delta F_1 \rangle$, and $E \langle w, \lambda^{-1} \Delta F_2 \rangle$), and Young's product inequality for the remaining cross terms. As expected, the gain in (85) is the same as the gain in (77). We next bound the loss and discretization error terms separately.

For the loss Λ in (86), apply the Peter-Paul inequality with parameter $(L\lambda^{-2})^{1/2}$, $\lambda h \leq 1$, and (76), to obtain

$$\begin{aligned}
\Lambda & \leq \lambda^{-1} \frac{K}{18} |z|^2 + \lambda^{-1} \frac{1}{18} |w|^2 \\
& + \lambda^{-1} \left(\frac{\lambda^3 h^3}{8} + \frac{\lambda^2 h^2}{2} + 2\lambda h + \frac{1}{2(L\lambda^{-2})^{1/2}} \left(\frac{\lambda^2 h^2}{4} + \frac{3\lambda h}{4} + 2 \right) \right) \lambda^{-2} E |\Delta F_u|^2 \\
& + \lambda^{-1} \left(\frac{\lambda h}{4} + \frac{(L\lambda^{-2})^{1/2}}{2} \left(\frac{\lambda^2 h^2}{4} + \frac{3\lambda h}{4} + 2 \right) \right) |w|^2 \\
& \stackrel{(67)}{\leq} \lambda^{-1} \frac{K}{18} |z|^2 + \lambda^{-1} \frac{1}{18} |w|^2 \\
& + \lambda^{-1} \left(\frac{21}{8} + \frac{3}{2(L\lambda^{-2})^{1/2}} \right) \lambda^{-2} E |\Delta F_u|^2 + \lambda^{-1} \left(\frac{1}{4} + \frac{3(L\lambda^{-2})^{1/2}}{2} \right) |w|^2 \\
& \stackrel{(76)}{\leq} \lambda^{-1} \frac{K}{18} |z|^2 + \lambda^{-1} \frac{1}{18} |w|^2
\end{aligned}$$

$$\begin{aligned}
& -\lambda^{-1} \left(\frac{21L\lambda^{-2}}{8} + \frac{3(L\lambda^{-2})^{1/2}}{2} \right) E\langle Z_{\mathcal{U}}, \Delta F_{\mathcal{U}} \rangle + \lambda^{-1} \left(\frac{1}{4} + \frac{3(L\lambda^{-2})^{1/2}}{2} \right) |w|^2 \\
(88) \quad & \stackrel{(66)}{\leq} -\lambda^{-1} \left(\frac{21}{8 \cdot 12^2} + \frac{1}{8} \right) E\langle Z_{\mathcal{U}}, \Delta F_{\mathcal{U}} \rangle + \lambda^{-1} \frac{K}{18} |z|^2 + \lambda^{-1} \frac{31}{72} |w|^2.
\end{aligned}$$

Combining (85) with (88), and following the corresponding steps in the proof of Lemma 20, we obtain

$$\begin{aligned}
\Gamma_0 + \Lambda & \leq \lambda^{-1} \left(\frac{137}{384} \right) E\langle Z_{\mathcal{U}}, \Delta F_{\mathcal{U}} \rangle + \lambda^{-1} \frac{K}{18} |z|^2 - \lambda^{-1} \frac{5}{72} |w|^2 \\
& \stackrel{(76)}{\leq} -\lambda^{-1} \left(\frac{137}{384} \right) KE|Z_{\mathcal{U}}|^2 + \lambda^{-1} \frac{K}{18} |z|^2 - \lambda^{-1} \frac{5}{72} |w|^2 \\
& \leq -\lambda^{-1} \left(\frac{137}{384} \right) K(|z|^2 + h\langle z, w \rangle + \frac{h^2}{3} |w|^2) + \lambda^{-1} \frac{K}{18} |z|^2 - \lambda^{-1} \frac{5}{72} |w|^2 \\
& \leq -\lambda^{-1} \left(\frac{137}{384} \right) K \left(\frac{1}{2} |z|^2 + \left(\frac{h^2}{3} - \frac{h^2}{2} \right) |w|^2 \right) + \lambda^{-1} \frac{K}{18} |z|^2 - \lambda^{-1} \frac{5}{72} |w|^2 \\
& \stackrel{(66)}{\leq} -\frac{1}{16} \lambda^{-1} (K|z|^2 + |w|^2) \stackrel{(64)}{\leq} -\frac{1}{16} \lambda^{-1} \min\left(\frac{12}{13} \lambda^2, K\right) \rho(y)^2 \\
(89) \quad & \leq -\frac{1}{18} \min(\lambda, K\lambda^{-1}) \rho(y)^2.
\end{aligned}$$

Note that the numerical pre-factors appearing in the last few steps were simplified for readability.

For the discretization error Δ in (87), apply $\lambda h \leq 1$, and insert (83) and (84),

$$\begin{aligned}
\Delta & = \left(\frac{\lambda^2 h^2}{8} + \frac{\lambda h}{4} + 36\lambda h \left(\frac{\lambda h}{8} + \frac{1}{8} \right)^2 + \frac{9\lambda h}{16K\lambda^{-2}} \right) \lambda^{-2} h E|\Delta F_1|^2 \\
& \quad + \left(2 + \frac{\lambda h}{4} \right) \lambda^{-2} h E|\Delta F_2|^2 + \lambda^{-1} \left(36 \left(1 + \frac{\lambda h}{4} \right)^2 + \frac{9}{4K\lambda^{-2}} \right) \lambda^{-2} |E\Delta F_2|^2 \\
& \stackrel{(67)}{\leq} \left(\frac{21}{8} + \frac{9}{16K\lambda^{-2}} \right) \lambda^{-2} h E|\Delta F_1|^2 + \left(\frac{9}{4} \right) \lambda^{-2} h E|\Delta F_2|^2 \\
& \quad + \lambda^{-1} \left(\frac{225}{4} + \frac{9}{4K\lambda^{-2}} \right) \lambda^{-2} |E\Delta F_2|^2 \\
& \leq 11 \left(\frac{39}{8} + \frac{9}{16K\lambda^{-2}} \right) (L\lambda^{-2}) L h^3 (L^2 h^2 |x|^2 + |v|^2) \\
& \quad + \frac{1}{12} \left(\frac{225}{4} + \frac{9}{4K\lambda^{-2}} \right) (L\lambda^{-2})^{3/2} L^{3/2} h^4 (L|x|^2 + |v|^2) \\
(90) \quad & \stackrel{(66)}{\leq} \frac{1}{2} \left(1 + \frac{1}{K\lambda^{-2}} \right) L h^3 (L^{3/2} h |x|^2 + |v|^2)
\end{aligned}$$

where in the last step several of the numerical pre-factors were rounded up to unity for readability.

Combining (89) and (90) gives (71) — as required. \square

REFERENCES

- [1] ACHLEITNER, F., ARNOLD, A. and STÜRZER, D. (2015). Large-time behavior in non-symmetric Fokker-Planck equations. *arXiv preprint arXiv:1506.02470*.

- [2] BLANES, S., CASAS, F. and SANZ-SERNA, J. M. (2014). Numerical integrators for the Hybrid Monte Carlo method. *SIAM Journal on Scientific Computing* **36** A1556–A1580.
- [3] BOU-RABEE, N. and EBERLE, A. (2020). Markov Chain Monte Carlo Methods. URL: <https://wt.iam.uni-bonn.de/eberle/>.
- [4] BOU-RABEE, N. and EBERLE, A. (2022). Couplings for Andersen Dynamics in High Dimension. *Ann. Inst. H. Poincaré Probab. Statist* **58** 916–944.
- [5] BOU-RABEE, N., EBERLE, A. and ZIMMER, R. (2020). Coupling and convergence for Hamiltonian Monte Carlo. *Ann. Appl. Probab.* **30** 1209–1250.
- [6] BOU-RABEE, N. and SANZ-SERNA, J. M. (2017). Randomized Hamiltonian Monte Carlo. *Ann. Appl. Probab.* **27** 2159–2194. <https://doi.org/10.1214/16-AAP1255>
- [7] BOU-RABEE, N. and SANZ-SERNA, J. M. (2018). Geometric Integrators and the Hamiltonian Monte Carlo Method. *Acta Numerica* **27** 113–206.
- [8] BOU-RABEE, N. and SCHUH, K. (2023). Convergence of unadjusted Hamiltonian Monte Carlo for mean-field models. *Electronic Journal of Probability* **28** 1 – 40.
- [9] CANCÉS, E., LEGOLL, F. and STOLTZ, G. (2007). Theoretical and Numerical Comparison of Some Sampling Methods for Molecular Dynamics. *Mathematical Modelling and Numerical Analysis* **41** 351–389.
- [10] CAO, Y., LU, J. and WANG, L. (2021). Complexity of randomized algorithms for underdamped Langevin dynamics. *Communications in Mathematical Sciences* **19** 1827–1853. <https://doi.org/10.4310/cms.2021.v19.n7.a4>
- [11] CASAS, F., SANZ-SERNA, J. M. and SHAW, L. (2023). A New Optimality Property of Strang’s Splitting. *SIAM Journal on Numerical Analysis* **61** 1369–1385.
- [12] CHEN, Y., DWIVEDI, R., WAINWRIGHT, M. J. and YU, B. (2020). Fast mixing of Metropolized Hamiltonian Monte Carlo: Benefits of multi-step gradients. *Journal of Machine Learning Research* **21** 1–72.
- [13] CHEN, Z. and VEMPALA, S. S. (2022). Optimal convergence rate of Hamiltonian Monte Carlo for strongly logconcave distributions. *Theory of Computing* **18** 1–18. <https://doi.org/10.4086/toc.2022.v018a009>
- [14] CHENG, X., CHATTERJI, N. S., ABBASI-YADKORI, Y., BARTLETT, P. L. and JORDAN, M. I. (2018). Sharp convergence rates for Langevin dynamics in the nonconvex setting. *arXiv preprint arXiv:1805.01648*.
- [15] CHENG, X., CHATTERJI, N. S., BARTLETT, P. L. and JORDAN, M. I. (2018). Underdamped Langevin MCMC: A non-asymptotic analysis. In *Conference On Learning Theory* 300–323.
- [16] DALALYAN, A. S. and RIOU-DURAND, L. (2020). On sampling from a log-concave density using kinetic Langevin diffusions. *Bernoulli* **26** 1956–1988.
- [17] DAUN, T. (2011). On the randomized solution of initial value problems. *Journal of Complexity* **27** 300–311. Dagstuhl 2009. <https://doi.org/10.1016/j.jco.2010.07.002>
- [18] DUANE, S., KENNEDY, A. D., PENDLETON, B. J. and ROWETH, D. (1987). Hybrid Monte-Carlo. *Phys Lett B* **195** 216–222.
- [19] DURMUS, A. and EBERLE, A. (2024). Asymptotic bias of inexact Markov Chain Monte Carlo methods in high dimension. *The Annals of Applied Probability* **34** 3435–3468.
- [20] DURMUS, A. and MOULINES, E. (2019). High-dimensional Bayesian inference via the unadjusted Langevin algorithm. *Bernoulli* **25** 2854–2882.
- [21] FANG, Y., SANZ-SERNA, J. M. and SKEEL, R. D. (2014). Compressible generalized hybrid Monte Carlo. *Journal of chemical physics* **140** 174108.
- [22] FOSTER, J., LYONS, T. and OBERHAUSER, H. (2021). The shifted ODE method for underdamped Langevin MCMC. <https://doi.org/10.48550/ARXIV.2101.03446>
- [23] HE, Y., BALASUBRAMANIAN, K. and ERDOGDU, M. A. (2020). On the Ergodicity, Bias and Asymptotic Normality of Randomized Midpoint Sampling Method. In *Advances in Neural Information Processing Systems* (H. LAROCHELLE, M. RANZATO, R. HADSELL, M. F. BALCAN and H. LIN, eds.) **33** 7366–7376. Curran Associates, Inc.
- [24] HOFFMAN, M. D. and GELMAN, A. (2014). The no-U-turn sampler: Adaptively setting path lengths in Hamiltonian Monte Carlo. *Journal of Machine Learning Research* **15** 1593–1623.
- [25] HOFFMAN, M. D. and SOUNTSOV, P. (2022). Tuning-Free Generalized Hamiltonian Monte Carlo. In *International Conference on Artificial Intelligence and Statistics* 7799–7813. PMLR.
- [26] KACEWICZ, B. (2004). Randomized and quantum algorithms yield a speed-up for initial-value problems. *Journal of Complexity* **20** 821–834. <https://doi.org/10.1016/j.jco.2004.05.002>
- [27] KACEWICZ, B. (2005). Almost Optimal Solution of Initial-Value Problems by Randomized and Quantum Algorithms. <https://doi.org/10.48550/ARXIV.QUANT-PH/0510045>
- [28] KLEPPE, T. S. (2022). Connecting the Dots: Numerical Randomized Hamiltonian Monte Carlo with State-Dependent Event Rates. *Journal of Computational and Graphical Statistics* **31** 1238–1253. <https://doi.org/10.1080/10618600.2022.2066679>

- [29] LEE, Y. T., SONG, Z. and VEMPALA, S. S. (2018). Algorithmic theory of ODEs and sampling from well-conditioned logconcave densities. *arXiv preprint arXiv:1812.06243*.
- [30] LU, J. and WANG, L. (2022). On explicit L 2-convergence rate estimate for piecewise deterministic Markov processes in MCMC algorithms. *Ann. Appl. Probab.* **32** 1333–1361.
- [31] MACKENZIE, P. B. (1989). An improved hybrid Monte Carlo method. *Physics Letters B* **226** 369–371.
- [32] MANGOUBI, O. and SMITH, A. (2021). Mixing of Hamiltonian Monte Carlo on strongly log-concave distributions: Continuous Dynamics. *Ann. Appl. Probab.* **31** 2019–2045.
- [33] MATTINGLY, J. C., STUART, A. M. and HIGHAM, D. J. (2002). Ergodicity for SDEs and approximations: locally Lipschitz vector fields and degenerate noise. *Stoch. Proc. Appl.* **101** 185–232.
- [34] MATTINGLY, J. C., STUART, A. M. and TRETYAKOV, M. V. (2010). Convergence of numerical time-averaging and stationary measures via Poisson equations. *SIAM J Num Anal* **48** 552–577.
- [35] MILSTEIN, G. N. and TRETYAKOV, M. V. (2021). *Mean-Square Approximation for Stochastic Differential Equations* In *Stochastic Numerics for Mathematical Physics* 1–94. Springer International Publishing, Cham.
- [36] MONMARCHÉ, P. (2022). HMC and underdamped Langevin united in the unadjusted convex smooth case. <https://doi.org/10.48550/ARXIV.2202.00977>
- [37] NEAL, R. M. (2011). MCMC using Hamiltonian dynamics. *Handbook of Markov Chain Monte Carlo* **2** 113–162.
- [38] QUISPEL, G. and MCLAREN, D. I. (2008). A new class of energy-preserving numerical integration methods. *Journal of Physics A: Mathematical and Theoretical* **41** 045206.
- [39] SANZ-SERNA, J. M. and STUART, A. M. (1999). Ergodicity of dissipative differential equations subject to random impulses. *Journal of Differential Equations* **155** 262–284.
- [40] SHEN, R. and LEE, Y. T. (2019). The randomized midpoint method for log-concave sampling. *Advances in Neural Information Processing Systems* **32**.
- [41] TALAY, D. (2002). Stochastic Hamiltonian Systems: Exponential Convergence to the Invariant Measure, and Discretization by the Implicit Euler Scheme. *Markov Processes and Related Fields* **8** 1–36.
- [42] VOGRINC, J. and KENDALL, W. S. (2021). Counterexamples for optimal scaling of Metropolis–Hastings chains with rough target densities. *Ann. Appl. Probab.* **31** 972–1019.
- [43] WU, L. (2001). Large and moderate deviations and exponential convergence for stochastic damping Hamiltonian systems. *Stochastic processes and their applications* **91** 205–238.